Inorganic Chemistry

FORUM ARTICLE

pubs.acs.org/IC

Harnessing Redox-Active Ligands for Low-Barrier Radical Addition at Oxorhenium Complexes

Cameron A. Lippert,[†] Kenneth I. Hardcastle,[‡] and Jake D. Soper*[,†]

[†]School of Chemistry and Biochemistry, Georgia Institute of Technology, Atlanta, Georgia 30332-0400, United States

[‡]X-ray Crystallography Center, Department of Chemistry, Emory University, 1515 Dickey Drive, Atlanta, Georgia 30322, United States

Supporting Information

ABSTRACT: The addition of an $[X]^+$ electrophile to the five-coordinate oxorhenium(V) anion $[Re^V(O)(ap^{Ph})_2]^-$ {$[ap^{Ph}]^{2-}$ = 2,4-di-*tert*-butyl-6-(phenylamido)phenolate} gives new products containing Re−X bonds. The Re−X bond-forming reaction is analogous to oxo transfer to $[Re^V(O)(ap^{Ph})_2]^-$ in that both are $2e^-$ redox processes, but the electronic structures of the products are different. Whereas oxo addition to $[Re^V(O)(ap^{Ph})_2]^-$ yields a closed-shell $[Re^{VII}(O)_2(ap^{Ph})_2]^-$ product of $2e^-$ metal oxidation, $[Cl]^+$ addition gives a diradical $Re^{VI}(O)(ap^{Ph})(isq^{Ph})Cl$ product ($[isq^{Ph}]^{\bullet-}$ = 2,4-di-*tert*-butyl-6-(phenylimino)semiquinonate) with $1e^-$ in a Re d orbital and $1e^-$ on a redox-active ligand. The differences in electronic structure are ascribed to differences in the π basicity of $[O]^{2-}$ and Cl^- ligands. The observation of ligand radicals in $Re^{VI}(O)(ap^{Ph})(isq^{Ph})X$ provides experimental support for the capacity of redox-active ligands to deliver electrons in other bond-forming reactions at $[Re^V(O)(ap^{Ph})_2]^-$, including radical additions of O_2 or TEMPO$^\bullet$ to make Re−O bonds. Attempts to prepare the electron-transfer series monomers between $Re^{VI}(O)(ap^{Ph})(isq^{Ph})X$ and $[Re^V(O)(ap^{Ph})_2]^-$ yielded a symmetric bis(μ-oxo)dirhenium complex. Formation of this dimer suggested that $Re^{VI}(O)(ap^{Ph})(isq^{Ph})Cl$ may be a source of an oxyl metal fragment. The ability of $Re^{VI}(O)(ap^{Ph})(isq^{Ph})Cl$ to undergo radical coupling at oxo was revealed in its reaction with $Ph_3C^\bullet$, which affords Ph_3COH and deoxygenated metal products. This reactivity is surprising because $Re^{VI}(O)(ap^{Ph})(isq^{Ph})Cl$ is not a strong outer-sphere oxidant or oxo-transfer reagent. We postulate that the unique ability of $Re^{VI}(O)(ap^{Ph})(isq^{Ph})Cl$ to effect oxo transfer to $Ph_3C^\bullet$ arises from symmetry-allowed mixing of a populated Re≡O π bond with a ligand-centered $[isq^{Ph}]^{\bullet-}$ ligand radical, which gives oxyl radical character to the oxo ligand. This allows the closed-shell oxo ligand to undergo a net $2e^-$ oxo-transfer reaction to $Ph_3C^\bullet$ via kinetically facile redox-active ligand-mediated radical steps. Harnessing intraligand charge transfer for radical reactions at closed-shell oxo ligands is a new strategy to exploit redox-active ligands for small-molecule activation and functionalization. The implications for the design of new oxidants that utilize low-barrier radical steps for selective multielectron transformations are discussed.

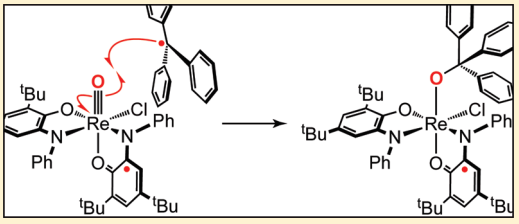

INTRODUCTION

Selectivity in most synthetically useful bond-making and bond-breaking redox reactions is predicated on maintaining $1e^-$ versus $2e^-$ redox control.[1−4] In this context, the utility of transition-metal catalysts for selective redox transformations of small molecules is usually a function of their ability to mediate the transfer of multiple electron equivalents while avoiding odd-electron intermediates.[5−7] For example, most organometallic catalysts feature later 4d and 5d transition metals because their tendency to maintain even d electron counts facilitates $2e^-$ redox steps for the selective activation and functionalization of organic substrates and inhibits deleterious $1e^-$ radical processes.[7−11]

Although catalysis involving free-radical intermediates has some synthetic utility,[1,12] free-radical reactions are more typically unselective, or selective for less valuable products. This is at least partly due to the fact that free-radical reactions often have very low kinetic barriers.[13] For that reason, harnessing low-barrier radical reactions for selective bond-making and -breaking is extremely desirable. For example, the ability of some metalloenzymes to mediate challenging small-molecule redox transformations has been attributed to their capacity to undergo radical reactions with the organic substrates without loss of specificity.[14−19] Selectivity in the biological redox systems is usually enforced by the protein structures, but mimicking secondary structure effects in synthetic systems can be challenging.[20−27] Accordingly, the development of new synthetic catalysts that can use free-radical reactions for small-molecule transformations will be predicated on elaborating new mechanisms to guide redox selectivity.

In recent years, the ability of some so-called "noninnocent" redox-active ligands to undergo low-energy intraligand or ligand−metal charge transfer (CT)[28,29] has found application in a range of stoichiometric and catalytic small-molecule activation and functionalization reactions.[7,21,30−53] Most of these recent successes exploit

Received: May 3, 2011
Published: July 11, 2011

Scheme 1

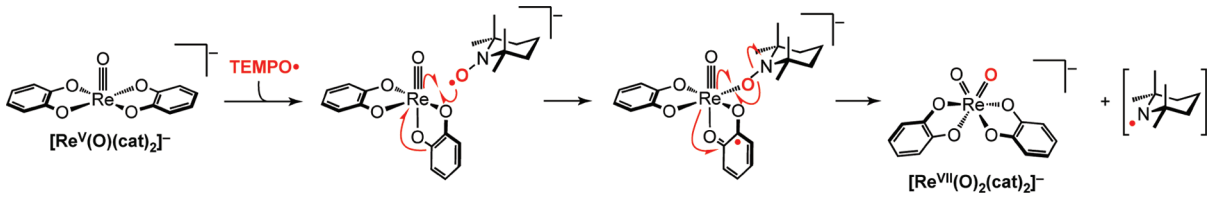

the capacity of redox-active ligand radicals to store and deliver charge to transition-metal ions for organometallic-type multielectron reactions at coordinatively unsaturated metal centers. Examples include $2e^-$ oxidative addition and reductive elimination reactions at redox-inert d^0 metals[30,32−37,44] or at naturally abundant late-first-row metal ions, which are more typically prone to $1e^-$ redox reactions.[39,41,48,50,53]

In another application of this strategy, we have shown that redox-active ligands mediate the deoxygenation of O_2 and nitroxyl radicals at five-coordinate oxorhenium(V) complexes $[Re^V(O)(L)_2]^-$ [where L^{2-} is 1,2-catecholate ($[cat]^{2-}$), tetrabromo-1,2-catecholate ($[Br_4cat]^{2-}$), 3,5-di-*tert*-butylcatecholate ($[3,5\text{-}^tBu_2cat]^{2-}$), or 2,4-di-*tert*-butyl-6-(phenylamido)phenolate ($[ap^{Ph}]^{2-}$)].[51,52] As shown in Scheme 1, ligand-centered redox activity was proposed to facilitate the net $2e^-$ oxo-transfer reactions by lowering the barrier to $1e^-$ Re−O bond formation, thereby circumventing high-energy oxorhenium(VI) intermediates. In these reactions, the propensity of oxorhenium centers to avoid odd-electron intermediates preserved the thermodynamic bias for $2e^-$ oxo transfer,[54] but the incorporation of an orthogonal ligand-centered $1e^-$ reservoir lowered the kinetic barrier to the reaction. Because attempts to isolate and experimentally characterize the kinetic products of $1e^-$ radical trapping were complicated by the comparative thermodynamic stability of the resulting $2e^-$-oxidized dioxo products $[Re^{VII}(O)_2(L)_2]^-$ (Scheme 1), evidence for ligand-radical intermediates came from computation and comparison of reaction rates among complexes with varying redox-active and redox-inert ligands.[51,52]

The capacity of redox-active ligands to undergo low-energy intraligand electron transfer (ET) has, to date, been less explored for redox reaction chemistry. Rather than supplying electrons for reactions at a coordinatively unsaturated metal center, we speculated that redox-active ligands on a coordinatively saturated metal could mediate redox reactions *at another ligand* in the same molecule. We were particularly intrigued by the idea of exploiting the intramolecular delocalization of a redox-active ligand free radical for radical addition at a terminal oxo group. In this context, the importance of unpaired spin on oxygen for radical reactions at terminal oxo ligands, including O−O bond formation and the activation of strong C−H bonds,[55−67] is still debated.[68−70]

This Forum Article revisits and expands on our earlier reports of oxidative bond-forming reactions at five-coordinate redox-active ligand oxorhenium(V) complexes.[51,52] The addition of a $[Cl]^+$ electrophile to $[Re^V(O)(ap^{Ph})_2]^-$ is shown to yield stable products with oxidized aminophenol ligands, providing experimental evidence for the capacity of redox-active ligands to be oxidized in Re−X bond-forming reactions. Data are additionally presented that suggest that the resulting six-coordinate oxorhenium complexes are susceptible to radical addition at the oxo ligand and that this reactivity arises from kinetic factors relating to the radical ligand ground state.

RESULTS

Preparation and Characterization of $Re^{VI}(O)(ap^{Ph})(isq^{Ph})X$ Complexes. To probe the potential intermediacy of redox-active ligand radicals in Re−O bond-forming reactions such as the one shown in Scheme 1, reactions of $[Re^V(O)(ap^{Ph})_2]^-$ {$[ap^{Ph}]^{2-}$ = 2,4-di-*tert*-butyl-6-(phenylamido)phenolate} were performed with oxidants that cannot form $[Re^{VII}(O)_2(ap^{Ph})_2]^-$. Treating a pale-green tetrahydrofuran solution of $(Et_4N)[Re^V(O)(ap^{Ph})_2]$ with 1 equiv of 2,3,4,5,6,6-hexachloro-2,4-cyclohexadien-1-one (which is a source of a $[Cl]^+$ electrophile)[71] under N_2 afforded an immediate color change to dark purple at 25 °C. The purple color corresponds to the formation of two air-stable rhenium products that are conveniently separated by column chromatography on silica gel. Matrix-assisted laser desorption ionization mass spectrometry (MALDI-MS) spectra of isolated materials showed molecular ion peaks at *m*/*z* 828 and 1058, corresponding to the molecular weights of the $[Re^V(O)(ap^{Ph})_2]^-$ reactant and a [Cl] or $[OC_6Cl_5]$ fragment, respectively (Scheme 2). The ratio of the two products varies with the reaction time and temperature. When a reaction mixture is chromatographed after 30 min at 25 °C, both the low-molecular-weight (14%) and high-molecular-weight species (35%) are formed in low yields. Heating the purple reaction mixture for 10 days at 60 °C increases the isolated yield of the *m*/*z* 1058 product to >70%, but the 12% yield of the *m*/*z* 828 product is effectively unchanged.

The slow evaporation of a saturated MeCN solution of the higher molecular weight product at 8 °C afforded purple crystals suitable for analysis by X-ray diffraction. A thermal ellipsoid plot is shown in Figure 1a. It contains a charge neutral six-coordinate oxorhenium center bound to one $[OC_6Cl_5]^-$ phenolate anion and two bidentate aminophenol-derived ligands. The geometry at rhenium is a distorted octahedron with the $[OC_6Cl_5]^-$ ligand cis to the oxo, giving the molecule C_1 symmetry and making the two aminophenol-derived chelates symmetry-inequivalent. Notably, examination of the aminophenol ligand bond distances reveals that they are also electronically inequivalent (Figure 1b). In the ligand trans to $[OC_6Cl_5]^-$, the C−C bond distances of the aminophenol ring are equidistant within 3σ at 1.40 ± 0.01 Å, and the C−O and C−N distances are 1.360(2) and 1.411(3) Å, respectively. These data are clearly consistent with a fully reduced $[ap^{Ph}]^{2-}$ ligand.[72,73] In contrast, the aminophenol ring in the ligand trans to the oxo has contracted C−O and C−N bond distances of 1.303(2) and 1.350(3) Å, and a quinoid-type pattern of four long and two short C−C bonds, so the metrical data best match those typical for the $[isq^{Ph}]^{\bullet-}$ radical monoanion {$[isq^{Ph}]^{\bullet-}$ = 2,4-di-*tert*-butyl-6-(phenylimino)semiquinonate}.[72,73] These ligand oxidation states imply that the complex is best formulated as $Re^{VI}(O)(ap^{Ph})(isq^{Ph})(OC_6Cl_5)$ containing a d^1 oxorhenium(VI) center.

The treatment of CH_2Cl_2 solutions of $Re^{VI}(O)(ap^{Ph})(isq^{Ph})(OC_6Cl_5)$ with excess aqueous HCl in air gives quantitative

dx.doi.org/10.1021/ic200923q |*Inorg. Chem.* 2011, 50, 9864–9878

Scheme 2

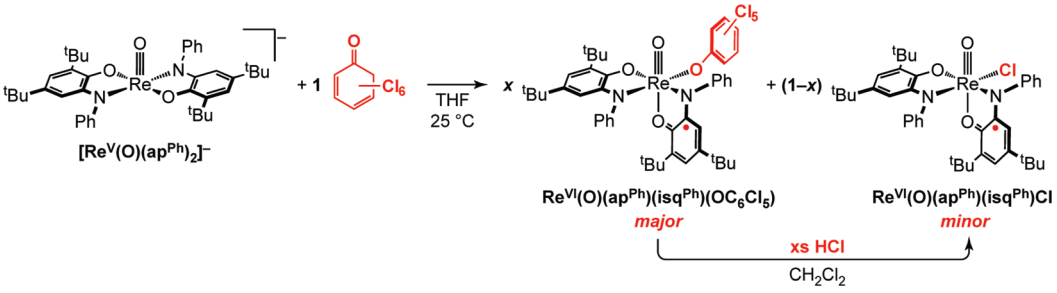

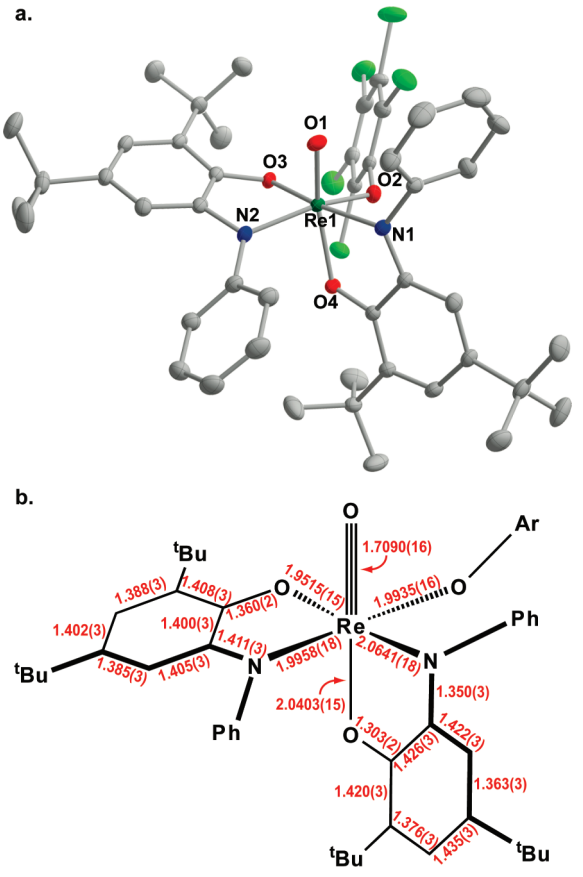

Figure 1. (a) Solid-state structure of one enantiomer of $Re^{VI}(O)(ap^{Ph})(isq^{Ph})(OC_6Cl_5)\cdot CH_3CN$ shown with 50% probability ellipsoids. The hydrogen atoms and CH_3CN solvate molecule are omitted for clarity. Both enantiomers cocrystallize and are observed in the X-ray structure. (b) Schematic of selected bond lengths (Å) drawn to correspond to part a. Selected bond angles (deg): O1−Re1−O4 157.07(7), O1−Re1−O3 95.47(7), O1−Re1−N1 85.22(7), O1−Re1−N2 96.81(8), O2−Re1−N1 87.53(7), O3−Re1−N2 79.71(7), O2−Re1−N2 153.38(8), O3−Re1−N1 170.09(7), N2−Re1−O4 82.67(7).

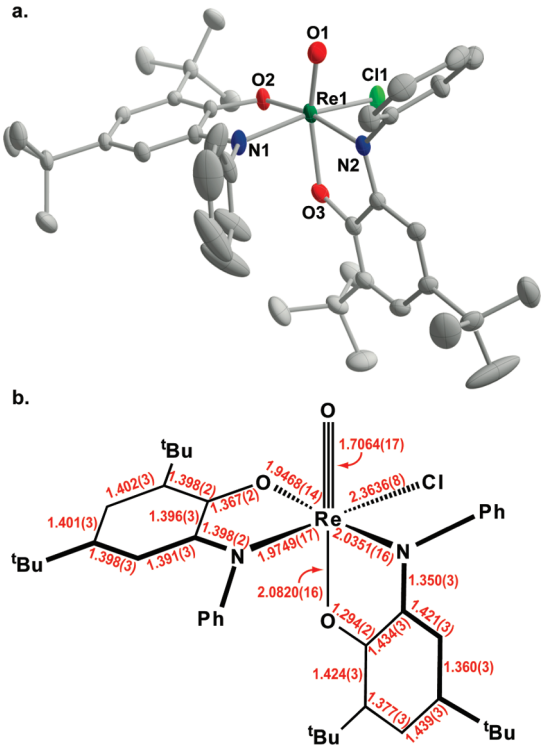

Figure 2. (a) Solid-state structure of one enantiomer of $Re^{VI}(O)(ap^{Ph})(isq^{Ph})Cl$ shown with 50% probability ellipsoids. The hydrogen atoms are omitted for clarity. Both enantiomers cocrystallize and are observed in the X-ray structure. (b) Schematic of selected bond lengths (Å) drawn to correspond to part a. Selected bond angles (deg): O1−Re1−O3 160.51(7), O1−Re1−O2 104.53(7), O1−Re1−N1 101.15(8), O1−Re1−N2 86.79(7), O1−Re1−Cl1 97.70(6), O2−Re1−N1 78.24(7), O2−Re1−N2 168.65(6), O1−Re1−Cl1 83.68(5), N2−Re1−Cl1 94.04(5), O2−Re1−O3 94.95 (6).

conversion to the low-molecular-weight product observed in the reaction of $[Re^{V}(O)(ap^{Ph})_2]^{-}$ with 2,3,4,5,6,6-hexachloro-2,4-cyclohexadien-1-one (Scheme 2). The identical product was independently synthesized by oxidation of $[Re^{V}(O)(ap^{Ph})_2]^{-}$ in CH_3CN using tris(4-bromophenyl)ammoniumyl hexachloroantimonate $[(C_6H_4Br)_3N][SbCl_6]$ at −20 °C. Crystals obtained from the latter procedure were analyzed by X-ray diffraction. As shown in Figure 2, the complex is the product of Cl^{-} for $[OC_6Cl_5]^{-}$ substitution at $Re^{VI}(O)(ap^{Ph})(isq^{Ph})(OC_6Cl_5)$. Consistent with their common core, the X-ray metrical data for the chloro complex strongly parallel those of the $Re^{VI}(O)(ap^{Ph})(isq^{Ph})(OC_6Cl_5)$ analogue. Because Cl^{-} occupies a site cis to the oxo ligand, the aminophenol ligands are symmetry-inequivalent, and their metrical data suggest that they are also in different oxidation states. The chelate bound trans to the oxo exhibits quinoid-type deviations from aromaticity and contracted C−O and C−N bond distances typical of an oxidized $[isq^{Ph}]^{\bullet-}$ radical, whereas the aminophenol ligand trans to Cl^{-} has metrical

dx.doi.org/10.1021/ic200923q |Inorg. Chem. 2011, 50, 9864–9878

Scheme 3

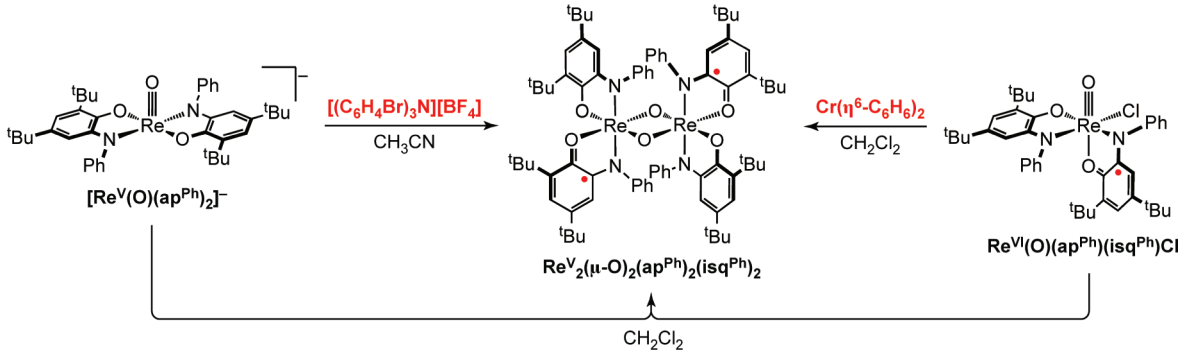

parameters consistent with dianionic $[ap^{Ph}]^{2-}$.[72,73] The complex is therefore best described as $Re^{VI}(O)(ap^{Ph})(isq^{Ph})Cl$, suggesting that substitution of Cl^- for $[OC_6Cl_5]^-$ does not significantly perturb the electronic structure of the $[Re^{VI}(O)(ap^{Ph})(isq^{Ph})]^+$ core.

The $Re^{VI}(O)(ap^{Ph})(isq^{Ph})X$ complexes are products of net $2e^-$ oxidation of $[Re^{V}(O)(ap^{Ph})_2]^-$, wherein $1e^-$ is removed from a redox-active amidophenolate ligand and $1e^-$ from a π-nonbonding metal orbital (d_{xy} when the $Re-O_{oxo}$ bond is coincident with the z axis). Accordingly, the $Re-O_{oxo}$ bond lengths of 1.7090(16) Å in $Re^{VI}(O)(ap^{Ph})(isq^{Ph})(OC_6Cl_5)$ and 1.7064(17) Å in $Re^{VI}(O)(ap^{Ph})(isq^{Ph})Cl$ are only very slightly contracted from the 1.715(3) Å $Re-O_{oxo}$ bond in $[Re^{V}(O)(ap^{Ph})_2]^-$, consistent with the expected Re≡O triple bond in all of the complexes.[74] In both complexes, formal $[X]^+$ addition occurs with the isomerization of two aminophenol ligands from an approximately trans disposition in $[Re^{V}(O)(ap^{Ph})_2]^-$ to a cis arrangement in $Re^{VI}(O)(ap^{Ph})(isq^{Ph})X$. In both cases, the ligand trans to the oxo group is oxidized.

Formulation of the $Re^{VI}(O)(ap^{Ph})(isq^{Ph})X$ complexes as a d^1 ions implies that they are diradicals at −100 °C in the solid state, with one unpaired electron on the metal and one localized on a free-radical $[isq^{Ph}]^{\bullet-}$ ligand. However, both $Re^{VI}(O)(ap^{Ph})(isq^{Ph})(OC_6Cl_5)$ and $Re^{VI}(O)(ap^{Ph})(isq^{Ph})Cl$ are diamagnetic. There is no measurable solution magnetic susceptibility by Evans' NMR method at 25 °C in CD_2Cl_2,[75,76] and the complexes exhibit sharp ^1H NMR resonances in the chemical shift ranges typical for diamagnetic molecules. Moreover, SQUID measurements of the solid-state susceptibility for $Re^{VI}(O)(ap^{Ph})(isq^{Ph})Cl$ were invariant over the range 4−400 K with $\chi_M \leq 1.5 \times 10^{-7}$ cm^3 mol^{-1}.

The ^1H NMR spectra of the $Re^{VI}(O)(ap^{Ph})(isq^{Ph})X$ complexes in CD_2Cl_2 show resonances for two unique aminophenol-derived ligands in each complex. Notably, a total of 10 resonances are observed for the two aminophenol *N*-phenyl substituents in $Re^{VI}(O)(ap^{Ph})(isq^{Ph})(OC_6Cl_5)$ at 25 °C, suggesting the rotation about the *N*-phenyl C−N bonds is locked. Similarly, the ^1H NMR spectrum of $Re^{VI}(O)(ap^{Ph})(isq^{Ph})Cl$ exhibits a mixture of broad and sharp *N*-phenyl resonances at 20 °C that separate into a 10-line pattern at −20 °C, also consistent with hindered rotation of the *N*-phenyl C−N bonds. In contrast, the ^1H NMR spectrum of the structurally related $[Re^{VII}(O)_2(ap^{Ph})_2]^-$ anion shows freely rotating *N*-aryl groups at 25 °C. Apparently, increasing the size of the sixth ligand on the $[Re^{VI}(O)(ap^{Ph})(isq^{Ph})]^+$ core, $[O]^{2-} < Cl^- < [OC_6Cl_5]^-$, results in steric congestion sufficient to hinder *N*-phenyl rotation.

Attempted Syntheses of $Re^{V}(O)(ap^{Ph})(isq^{Ph})$ and $[Re^{V}(O)(ap^{Ph})(isq^{Ph})Cl]^-$. Our initial efforts to prepare the product of $1e^-$ oxidation of $[Re^{V}(O)(ap^{Ph})_2]^-$ using tris(4-bromophenyl)ammoniumyl hexachloroantimonate $[(C_6H_4Br)_3N][SbCl_6]$ instead gave low-yield conversion to the $2e^-$-oxidized $Re^{VI}(O)(ap^{Ph})(isq^{Ph})Cl$ (vide supra). However, the addition of 1 equiv of the tetrafluoroborate salt of the same oxidant $[(C_6H_4Br)_3N][BF_4]$ to $[Re^{V}(O)(ap^{Ph})_2]^-$ in CH_3CN resulted in the immediate precipitation of a dark-purple powder. MALDI-MS analysis of the purple solids showed a weak molecular ion peak at 1586 m/z and a base peak at half of the mass of the parent ion, m/z 793, the same molecular weight as that of the $[Re^{V}(O)(ap^{Ph})_2]^-$ starting material. The same product was obtained by two complementary routes (Scheme 3): (1) reduction of $Re^{VI}(O)(ap^{Ph})(isq^{Ph})Cl$ using 1 equiv of bis(benzene)chromium $[Cr(\eta^6\text{-}C_6H_6)_2]$ in CH_2Cl_2; (2) stoichiometric reaction of $[Re^{V}(O)(ap^{Ph})_2]^-$ with $Re^{VI}(O)(ap^{Ph})(isq^{Ph})Cl$ in CH_2Cl_2. Solids obtained by all three methods gave identical UV−vis absorption spectra and MALDI-MS spectra. Additionally, single crystals obtained from each of the independent syntheses were analyzed by X-ray crystallography. Although all crystals yielded only low-quality data, the structures were sufficient to assign atom connectivity, confirming that only one product is formed in all three reactions. A plot of a representative single-crystal data set is shown in Figure 3. The complex is a charge neutral bis(μ-oxo)dirhenium complex where the coordination sphere of each rhenium ion is completed by two aminophenol ligands. Formation of the bis(μ-oxo) dimer requires one of the two trans $[ap^{Ph}]^{2-}$ ligands in $[Re^{V}(O)(ap^{Ph})_2]^-$ to twist into a cis conformation. This isomerization places the oxygen donors from $[ap^{Ph}]^{2-}$-derived ligands in the sites trans to the diamond-core bridging oxos, consistent with their preferred orientation in the $[Re^{VII}(O)_2(ap^{Ph})_2]^-$ and $Re^{VI}(O)(ap^{Ph})(isq^{Ph})X$ complexes, making all of the Re−O bonds approximately coplanar.

The bis(μ-oxo)dirhenium complex is the net product of $1e^-$ oxidation of two $[Re^{V}(O)(ap^{Ph})_2]^-$ anions followed by dimerization of the resulting charge neutral monomers. The immediate product of $1e^-$ oxidation of $S = 0$ $[Re^{V}(O)(ap^{Ph})_2]^-$ is necessarily a charge-neutral $S = {}^1/_2$ radical monomer, so assuming a symmetric charge distribution, dimerization should yield a diradical product. The isolated bis(μ-oxo)dirhenium species is $S = 0$, as evidenced by its diamagnetic ^1H NMR spectrum in CD_2Cl_2 and C_6D_6, suggesting that the two unpaired electrons are strongly antiferromagnetically coupled. The removal of $1e^-$ from $[Re^{V}(O)(ap^{Ph})_2]^-$ could result in either a metal- or ligand-centered oxidation. If the oxidation is ligand-centered, the dimer

dx.doi.org/10.1021/ic200923q |*Inorg. Chem.* 2011, 50, 9864–9878

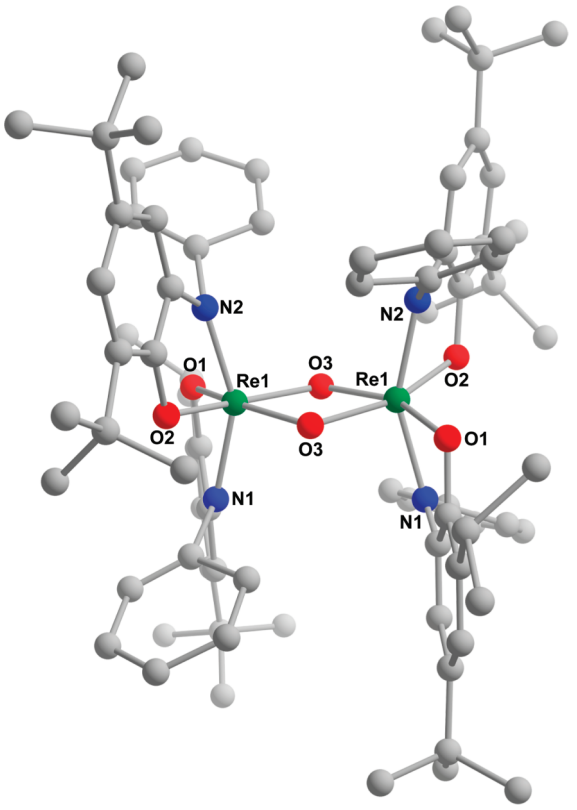

Figure 3. Ball-and-stick representation of the solid-state data from a single crystal of $Re^{V}_2(\mu\text{-}O)_2(ap^{Ph})_2(isq^{Ph})_2$. The hydrogen atoms are omitted for clarity. All attempted syntheses yielded only low-quality, twinned crystals, so the oxygen and nitrogen atoms were solved isotropically. The data shown are sufficient to establish atom connectivity but not to assign ligand oxidation states.

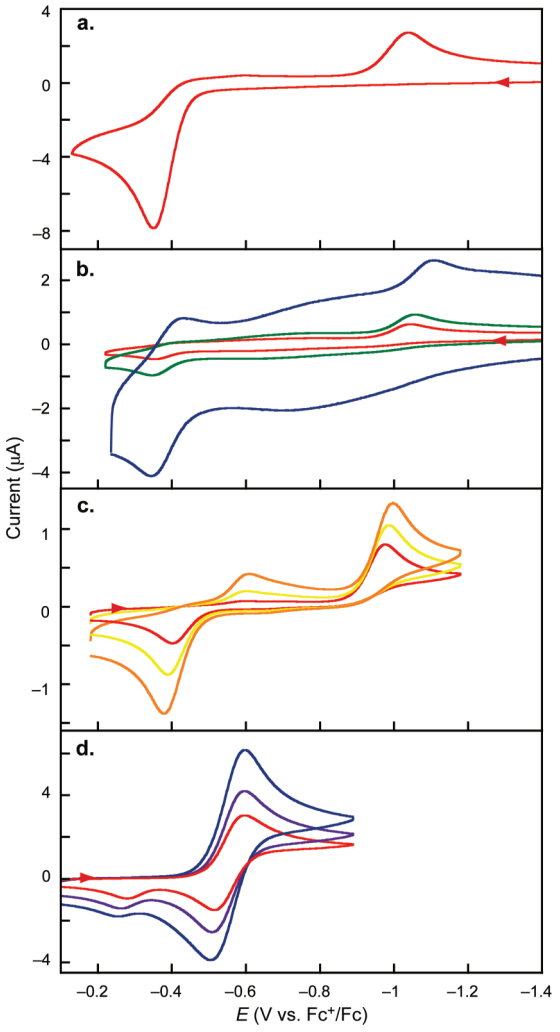

Figure 4. Cyclic voltammograms of (a) $(Et_4N)[Re^{V}(O)(ap^{Ph})_2]$ in CH_3CN containing 0.1 M $[^nBu_4N][PF_6]$ at 100 mV s^{-1} scan rate. (b) $Re^{V}_2(\mu\text{-}O)_2(ap^{Ph})_2(isq^{Ph})_2$ in CH_2Cl_2 containing 0.1 M $[^nBu_4N][PF_6]$ at 100 (red), 250 (green), and 2000 (blue) mV s^{-1} scan rate. (c) $Re^{V}_2(\mu\text{-}O)_2(ap^{Ph})_2(isq^{Ph})_2$ in CH_2Cl_2 containing 0.1 M $[^nBu_4N]Cl$ at 25 (red), 50 (yellow), and 100 (orange) mV s^{-1} scan rate. (d) $Re^{VI}(O)(ap^{Ph})(isq^{Ph})Cl$ in CH_3CN containing 0.1 M $[^nBu_4N]Cl$ at 50 (red), 100 (purple), and 250 (blue) mV s^{-1} scan rate. All cyclic voltammetry scans were measured at 25 °C using a 10 mm Pt electrode.

is $Re^{V}_2(\mu\text{-}O)_2(ap^{Ph})_2(isq^{Ph})_2$, whereas a metal-centered oxidation product gives $Re^{VI}_2(\mu\text{-}O)_2(ap^{Ph})_4$. Although the latter, d^1-d^1, formulation could explain the observed diamagnetism of the dimer via the formation of a Re−Re single bond,[77] the observed Re−Re distance of 3.0223(9) Å is much longer than other edge-sharing bioctahedral bis(μ-oxo) complexes containing a metal−metal bond (ca. 2.5−2.6 Å).[78] An alternative through-bond pathway for radical coupling to yield the $S = 0$ dimer ground state invokes radical delocalization onto the bridging oxo ligands. The large experimental error associated with the dimer Re−O bond distances prevents structural analysis of the Re−O_{oxo} bonding, which may be indicative of such delocalization. However, as discussed below, intramolecular electron delocalization into the Re−O_{oxo} bond is similarly invoked to rationalize radical addition reactions at the oxo ligand in $Re^{VI}(O)(ap^{Ph})(isq^{Ph})Cl$. For the remainder of this manuscript, we use the ligand-centered oxidation $Re^{V}_2(\mu\text{-}O)_2(ap^{Ph})_2(isq^{Ph})_2$ formulation, for reasons highlighted later, but $Re^{VI}_2(\mu\text{-}O)_2(ap^{Ph})_4$ is equally consistent with the available experimental data.

Cyclic voltammograms of $[Re^{V}(O)(ap^{Ph})_2]^-$, $Re^{V}_2(\mu\text{-}O)_2(ap^{Ph})_2(isq^{Ph})_2$, and $Re^{VI}(O)(ap^{Ph})(isq^{Ph})Cl$ are shown in Figure 4. In CH_3CN with a $[^nBu_4N][PF_6]$ supporting electrolyte, irreversible oxidation of $[Re^{V}(O)(ap^{Ph})_2]^-$ occurs at E_{pa} = −0.35 V versus Fc^+/Fc (Figure 4a). A cathodic wave of lower current density is observed at E_{pc} = −1.03 V. The voltammogram for isolated $Re^{V}_2(\mu\text{-}O)_2(ap^{Ph})_2(isq^{Ph})_2$ in CH_2Cl_2 with a $[^nBu_4N][PF_6]$ electrolyte (Figure 4b) is nearly identical, except at fast scan rates (>2.0 V s^{-1}) a second cathodic wave appears at E_{pc} = −0.43 V.[79] These data imply that $Re^{V}_2(\mu\text{-}O)_2(ap^{Ph})_2(isq^{Ph})_2$ and $[Re^{V}(O)(ap^{Ph})_2]^-$ are rapidly interconverted on the electrochemical time scale via a so-called EC_{dim} process:[80] The oxidation of $[Re^{V}(O)(ap^{Ph})_2]^-$ leads to dimerization to $Re^{V}_2(\mu\text{-}O)_2(ap^{Ph})_2(isq^{Ph})_2$ and the reduction of $Re^{V}_2(\mu\text{-}O)_2(ap^{Ph})_2(isq^{Ph})_2$ results in dissociation of the dimer to regenerate the monomeric $[Re^{V}(O)(ap^{Ph})_2]^-$ anion. At fast scan rates (Figure 4b, blue line), the oxidation of $[Re^{V}(O)(ap^{Ph})_2]^-$ becomes quasi-reversible because the rereduction of the $1e^-$-oxidized $Re^{V}(O)(ap^{Ph})(isq^{Ph})$ monomer becomes competitive with dimerization to make $Re^{V}_2(\mu\text{-}O)_2(ap^{Ph})_2(isq^{Ph})_2$. Although quantitative values for both the rate of dimerization and K_{dim} should be obtainable via digital simulation of the electrochemical data, a previous report has noted that extraction of the thermodynamic and kinetic data for an EC_{dim} process is challenging when the monomer/dimer equilibrium lies strongly toward the products,

as is the case here.[80] This is exacerbated by differences in the solubilities of $[Re^{V}(O)(ap^{Ph})_2]^-$ and $Re^{V}_2(\mu\text{-}O)_2(ap^{Ph})_2(isq^{Ph})_2$, which affect the voltammograms. For instance, the cathodic current for the reduction of $Re^{V}_2(\mu\text{-}O)_2(ap^{Ph})_2(isq^{Ph})_2$ in CH_3CN (Figure 4a) is likely decreased relative to the anodic current density because $Re^{V}_2(\mu\text{-}O)_2(ap^{Ph})_2(isq^{Ph})_2$ precipitates rapidly from CH_3CN.

To probe whether chloride is a suitable trap of $Re^{V}(O)(ap^{Ph})(isq^{Ph})$, cyclic voltammograms of $Re^{V}_2(\mu\text{-}O)_2(ap^{Ph})_2(isq^{Ph})_2$ were obtained in CH_2Cl_2 with a $[^nBu_4N]Cl$ electrolyte (Figure 4c). At slower scan rates (ca. 50 mV s^{-1}), the data mirror those in Figure 4a,b. Interestingly, at faster scan rates (100−250 mV s^{-1}), the reduction of $Re^{V}_2(\mu\text{-}O)_2(ap^{Ph})_2(isq^{Ph})_2$ is preceded by a small prewave at $E_{pc} = -0.60$ V. We initially suspected that this might correspond to the reduction of a coordinatively saturated $[Re^{V}(O)(ap^{Ph})(isq^{Ph})Cl]^-$ complex. However, the cyclic voltammogram of isolated $Re^{VI}(O)(ap^{Ph})(isq^{Ph})Cl$ in CH_3CN (Figure 4d) shows only a quasi-reversible reduction centered at −0.55 V versus Fc^+/Fc. Because $Re^{VI}(O)(ap^{Ph})(isq^{Ph})Cl$ does not react with ferrocene but is reduced by $Cr(\eta^6\text{-}C_6H_6)_2$ (with a reduction potential of −1.15 V in CH_2Cl_2),[81] the electrochemical event at −0.55 V in Figure 4d can be assigned to the interconversion of $Re^{VI}(O)(ap^{Ph})(isq^{Ph})Cl$ and $[Re^{V}(O)(ap^{Ph})(isq^{Ph})Cl]^-$. Notably, increasing scan rates cause the ratio of cathodic and anodic current densities in Figure 4d to approach unity as the reaction becomes more reversible.

The sum of these electrochemical data yields two conclusions: (1) Cl^- binding to $Re^{V}(O)(ap^{Ph})(isq^{Ph})$ is both thermodynamically weak and kinetically slow. Even in the presence of a large excess of Cl^-, the formation of $Re^{V}(O)(ap^{Ph})(isq^{Ph})$ is followed by rapid dimerization to $Re^{V}_2(\mu\text{-}O)_2(ap^{Ph})_2(isq^{Ph})_2$. A $[Re^{V}(O)(ap^{Ph})(isq^{Ph})Cl]^-$ transient can be observed from the reduction of $Re^{VI}(O)(ap^{Ph})(isq^{Ph})Cl$ in Figure 4d, presumably because Cl^- is already in the coordination sphere. However, under the same conditions (with the same excess Cl^-), the oxidation of $[Re^{V}(O)(ap^{Ph})_2]^-$ does not give any observable $[Re^{V}(O)(ap^{Ph})(isq^{Ph})Cl]^-$, implying that Cl^- is a kinetically poor trap of the $Re^{V}(O)(ap^{Ph})(isq^{Ph})$ monomer. (2) The "prewave" at $E_{pc} = -0.60$ V in Figure 4c is not due to the reduction of $[Re^{V}(O)(ap^{Ph})(isq^{Ph})Cl]^-$. Because $Re^{VI}(O)(ap^{Ph})(isq^{Ph})Cl$ is reduced at $E_{pc} = -0.59$ V, the reduction of the chloro-bound anion $[Re^{V}(O)(ap^{Ph})(isq^{Ph})Cl]^-$ would require a potential substantially below −0.60 V. It is possible that the prewave corresponds to the formation of $Re^{VI}(O)(ap^{Ph})(isq^{Ph})Cl$, but it is not clear why this product would be preferred at faster scan rates.

These electrochemical conclusions are supported by the chemical redox experiments. The formation of $Re^{V}_2(\mu\text{-}O)_2(ap^{Ph})_2(isq^{Ph})_2$ by the reduction or comproportionation methods described above (Scheme 3) requires a loss of 2 or 1 equiv of Cl^-, respectively, implying that the putative monomeric $[Re^{V}(O)(ap^{Ph})(isq^{Ph})Cl]^-$ anion has a low affinity for Cl^-. Furthermore, the UV−vis absorption spectrum of isolated $Re^{V}_2(\mu\text{-}O)_2(ap^{Ph})_2(isq^{Ph})_2$ in CH_2Cl_2 is unchanged with excess [PPN]Cl {$[PPN]^+$ = bis(triphenylphosphoranylidene)ammonium} or pyridine, suggesting that the bis(μ-oxo) complex is the thermodynamic minimum on the ET series between $[Re^{V}(O)(ap^{Ph})_2]^-$ and $Re^{VI}(O)(ap^{Ph})(isq^{Ph})Cl$. Finally, oxidations of $[Re^{V}(O)(ap^{Ph})_2]^-$ preformed in the presence of a large excess of Cl^- salts give $Re^{V}_2(\mu\text{-}O)_2(ap^{Ph})_2(isq^{Ph})_2$ at the same fast apparent rate as those without added Cl^-.

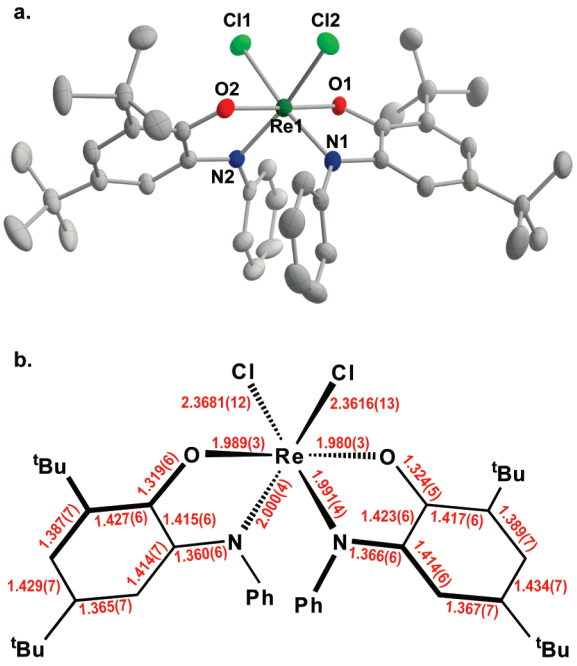

Figure 5. (a) Solid-state structure of $Re^{V}(ap^{Ph})(isq^{Ph})Cl_2 \cdot 0.65\text{-}CH_2Cl_2$ shown with 50% probability ellipsoids. The hydrogen atoms and CH_2Cl_2 solvate are omitted for clarity. (b) Schematic of selected bond lengths (Å) drawn to correspond to Figure 5a. Selected bond angles (deg): O1−Re1−O2 178.84(3), O1−Re1−Cl1 91.19(9), O1−Re1−Cl2 89.25(10), O1−Re1−N2 103.04(14), O2−Re1−N1 103.18(14), N1−Re1−Cl1 167.86(11), N1−Re1−Cl2 89.02(12).

Consistent with these observations, all attempts to isolate $[Re^{V}(O)(ap^{Ph})(isq^{Ph})Cl]^-$ by the chemical oxidation of $[Re^{V}(O)(ap^{Ph})_2]^-$ in the presence of Cl^- or by the direct addition of $Cl^{\bullet}$ were unsuccessful. Heating CH_2Cl_2 solutions of $[Re^{V}(O)(ap^{Ph})_2]^-$ with 2.4 equiv of Me_3SiCl at 65 °C instead afforded an new air-stable maroon product, which was conveniently purified by chromatography on silica gel. Single crystals of the dark-red material were obtained from a concentrated CH_2Cl_2 solution and analyzed by X-ray diffraction. A thermal ellipsoid plot is provided in Figure 5a. It shows a charge-neutral six-coordinate rhenium ion with two chloro ligands and two crystallographically unique aminophenol-derived ligands. The aminophenol Re−O bonds are in an approximately trans disposition, placing the two chloro ligands in cis sites and giving the pseudooctahedral rhenium approximate C_2 symmetry. Bond distances are collected in Figure 5b. The C−N and C−O bonds average 1.36 and 1.32 Å, respectively. These are longer than the $[isq^{Ph}]^{\bullet-}$ ligands in the $Re^{VI}(O)(ap^{Ph})(isq^{Ph})X$ complexes but shorter than the $[ap^{Ph}]^{2-}$ ligand distances (Figures 1 and 2). Moreover, the C−C bonds exhibit a small but significant quinoid distortion from aromaticity. In total, the distances are in good agreement with the arithmetic mean of those expected for the $[ap^{Ph}]^{2-}$ and $[isq^{Ph}]^{\bullet-}$ ligand oxidation states.[72,73] This suggests that the complex is best described as $Re^{V}(ap^{Ph})(isq^{Ph})Cl_2$ containing a single ligand-centered unpaired electron. Evidence for a $S = {}^1/_2$ assignment is provided by the solution magnetic moment of 1.77 μ_B at 25 °C in CD_3CN and the absence of any well-resolved resonances in the ^1H NMR spectrum. Note that this formulation does not delineate whether the structure has electronic asymmetry, with the unpaired electron localized on a single $[isq^{Ph}]^{\bullet-}$ ligand, or whether the electron is delocalized

dx.doi.org/10.1021/ic200923q |Inorg. Chem. 2011, 50, 9864–9878

Scheme 4

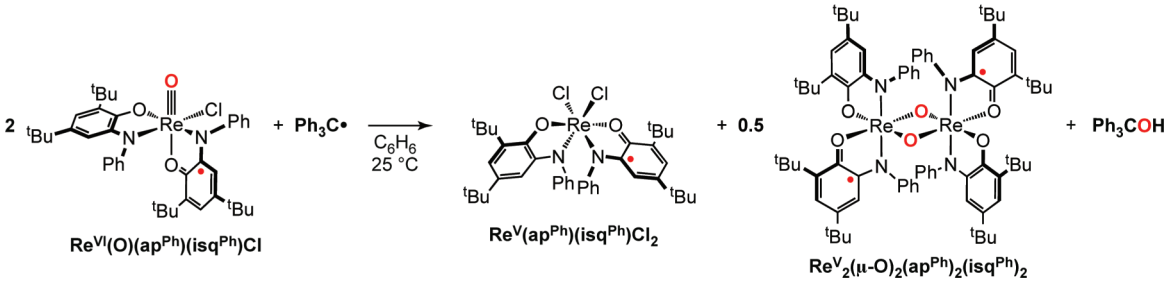

across both of the aminophenol ligands. The X-ray data are consistent with either possibility.

Re(O)(ap^{Ph})(isq^{Ph})Cl Oxo Transfer to PhC$^{\bullet}$. Treating Re^{VI}(O)(ap^{Ph})(isq^{Ph})Cl with 1.1 equiv of triphenylmethyl radical Ph$_3$C$^{\bullet}$ in C$_6$H$_6$, with exclusion of ambient light, results in a slow color change from violet to red-purple over 1 week at 25 °C. To limit deleterious side reactions of the free radical,[82] the reaction was performed with stoichiometric Ph$_3$C$^{\bullet}$. However, the true concentration of the free Ph$_3$C$^{\bullet}$ radical in C$_6$H$_6$ is only 2% of the Gomberg dimer,[83,84] so for the majority of the reaction, the concentration of dissolved Re^{VI}(O)(ap^{Ph})(isq^{Ph})Cl was large relative to the solution [Ph$_3$C$^{\bullet}$] concentration. Gas chromatography−mass spectrometry (GC−MS) analysis of the reaction mixtures revealed that triphenylmethanol Ph$_3$COH is the major product, formed in 69% yield based on limiting rhenium (Figure S1 in the Supporting Information). Minor products in GC−MS include benzophenone and triphenylmethane, which make up <10% of the total of Ph$_3$C$^{\bullet}$-derived materials. The red-purple reaction mixture contains three rhenium products. These are an unreacted Re^{VI}(O)(ap^{Ph})(isq^{Ph})Cl starting material, as well as Re^{V}(ap^{Ph})(isq^{Ph})Cl$_2$ and Re$^{V}_2$(μ-O)$_2$(ap^{Ph})$_2$(isq^{Ph})$_2$. The identity of each was confirmed by the isolation and comparison of UV−vis absorption spectra to the authentic materials prepared independently. In total, the yields of all of the organic and rhenium products are in excellent agreement with the oxo-transfer reaction stoichiometry shown in Scheme 4. In contrast, treating Re^{VI}(O)(ap^{Ph})(isq^{Ph})Cl with excess PPh$_3$ (ca. 20 equiv) does not give OPPh$_3$ or deoxygenated rhenium products over days at ambient temperature, suggesting that Re^{VI}(O)(ap^{Ph})(isq^{Ph})Cl is not a strong thermodynamic oxo donor.[85,86]

The immediate product of net oxo transfer from Re^{VI}(O)(ap^{Ph})(isq^{Ph})Cl to Ph$_3$C$^{\bullet}$ is a triphenylmethoxyl Ph$_3$CO$^{\bullet}$ radical. However, this species is known to undergo a rapid 1,2-phenyl shift to yield the α-phenoxydiphenylmethyl radical.[87] Accordingly, our observation of the high-yield formation of Ph$_3$COH suggests that the free Ph$_3$CO$^{\bullet}$ radical is not an intermediate in the oxidation. The generation of Ph$_3$COH in Scheme 4 requires the net addition of 1 equiv of H$^{\bullet}$; the source of this adventitious H$^{\bullet}$ is unknown. Control reactions confirmed that Ph$_3$COH is not obtained from exposure of Ph$_3$C$^{\bullet}$ to O$_2$ under conditions analogous to those employed in Scheme 4. Furthermore, oxo transfer to make Ph$_3$COH is not a general feature of the oxorhenium complexes used in this study. For example, the UV−vis spectrum of the bis(μ-oxo) dimer Re$^{V}_2$(μ-O)$_2$(ap^{Ph})$_2$(isq^{Ph})$_2$ in C$_6$H$_6$ is unchanged with stoichiometric or excess Ph$_3$C$^{\bullet}$ or [Ph$_3$C][BF$_4$] (1−30 equiv per rhenium) over 2−6 days at ambient temperature; no Ph$_3$COH is observed by GC−MS from any of the reactions. Mixing 1 equiv of Ph$_3$C$^{\bullet}$ with [Re^{V}(O)(ap^{Ph})$_2$]$^{-}$ in C$_6$H$_6$ gave slow conversion to a slightly darker yellow-green solution that contained ca. 15−30% of the 1e^{-} oxidation product Re$^{V}_2$(μ-O)$_2$(ap^{Ph})$_2$(isq^{Ph})$_2$ but no Ph$_3$COH. The addition of 1 equiv of [Ph$_3$C][BF$_4$] of a C$_6$H$_6$ solution of [Re^{V}(O)(ap^{Ph})$_2$]$^{-}$ afforded an immediate color change from pale yellow-green to purple. Analysis of the reaction mixture by UV−vis spectroscopy and MALDI-MS after 24 h at ambient temperature confirmed that the purple color corresponded to the generation of Re$^{V}_2$(μ-O)$_2$(ap^{Ph})$_2$(isq^{Ph})$_2$ in 90% isolated yield based on rhenium, suggesting that the Ph$_3$C^{+} cation is a competent 1e^{-} oxidant for [Re^{V}(O)(ap^{Ph})$_2$]$^{-}$. As illustrated in eq 1, the reduced product of this reaction is presumably Ph$_3$C$^{\bullet}$. The lack of any Ph$_3$COH product in GC−MS is consistent with the proposed product distribution because, as described above, Re$^{V}_2$(μ-O)$_2$(ap^{Ph})$_2$(isq^{Ph})$_2$ is inert to Ph$_3$C$^{\bullet}$. Finally, exposure of a 90:10 C$_6$H$_6$/CH$_3$CN solution of [Re^{VII}(O)$_2$(ap^{Ph})$_2$]$^{-}$ to 1 equiv of Ph$_3$C$^{\bullet}$ gives no obvious color change and no Ph$_3$COH by GC−MS. The implications of these results for the mechanism of oxo transfer in Scheme 4 are discussed below.

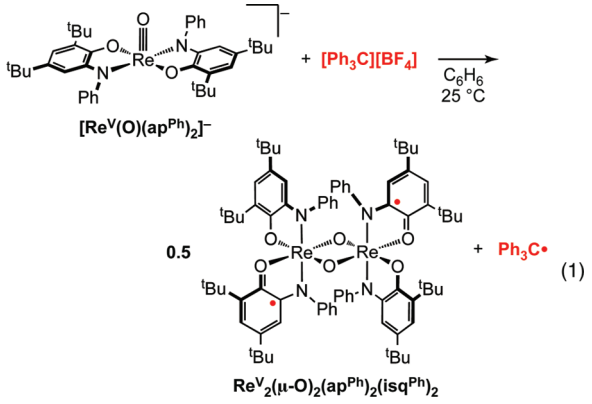

(1)

DISCUSSION

Ligand Radicals in Re−X Bond-Forming Reactions. The addition of a [Cl]$^{+}$ electrophile to [Re^{V}(O)(ap^{Ph})$_2$]$^{-}$ to make Re^{VI}(O)(ap^{Ph})(isq^{Ph})Cl is a 2e^{-} redox process that parallels oxo transfer to [Re^{V}(O)(ap^{Ph})$_2$]$^{-}$ to generate [Re^{VII}(O)$_2$(ap^{Ph})$_2$]$^{-}$.[51] In both reactions, formation of the new Re−X bond occurs cis to the oxo ligand, requiring isomerization of the [ap^{Ph}]$^{2-}$ ligands to a cis orientation. The X-ray structures of [Re^{VII}(O)$_2$(ap^{Ph})$_2$]$^{-}$ and both Re^{VI}(O)(ap^{Ph})(isq^{Ph})X complexes provide evidence for the torsional flexibility of the [Re^{V}(O)(ap^{Ph})$_2$]$^{-}$ core and the capacity of the [ap^{Ph}]$^{2-}$ ligands to achieve a cis conformation. However, their ^{1}H NMR data suggest that the cis conformer is sterically congested, and increasing steric pressure with substitution of

dx.doi.org/10.1021/ic200923q |Inorg. Chem. 2011, 50, 9864–9878

$[O]^{2-}$ for Cl^- or $[OC_6Cl_5]^-$ challenges the capacity of the $[Re^{VI}(O)(ap^{Ph})(isq^{Ph})]^+$ core to accommodate the larger X^- ligands. It is likely that this steric hindrance is a factor in the instability of the $[Re^{V}(O)(ap^{Ph})(isq^{Ph})Cl]^-$ monomer.

Both $[Cl]^+$ and oxo addition to $[Re^{V}(O)(ap^{Ph})_2]^-$ give products of net $2e^-$ oxidation, but the electronic structures of the rhenium products are different. As implied by the formulas, generation of $[Re^{VII}(O)_2(ap^{Ph})_2]^-$ removes $2e^-$ from the oxorhenium(V) center in $[Re^{V}(O)(ap^{Ph})_2]^-$ but the formation of $Re^{VI}(O)(ap^{Ph})(isq^{Ph})Cl$ removes $1e^-$ from the metal and $1e^-$ from a redox-active $[ap^{Ph}]^{2-}$ ligand. This description makes $Re^{VI}(O)(ap^{Ph})(isq^{Ph})Cl$ a diradical, with one unpaired electron in a Re d orbital and one on a free radical $[isq^{Ph}]^{\bullet-}$ ligand. However, the diamagnetism of $Re^{VI}(O)(ap^{Ph})(isq^{Ph})Cl$ suggests that the unpaired spins are strongly antiferromagnetically coupled. We favor this charge-localized description but note that, in the strong coupling limit, the diradical formulation is equivalent to a closed-shell model with a single doubly occupied molecular orbital comprised of both a metal d orbital and a redox-active aminophenol ligand π^* orbital. The differences in the electronic structures of $[Re^{VII}(O)_2(ap^{Ph})_2]^-$ and $Re^{VI}(O)(ap^{Ph})(isq^{Ph})Cl$ can be rationalized by considering the relative π-donor abilities of Cl^- versus $[O]^{2-}$. Cis dioxo complexes in tetragonal fields are d^0 to minimize repulsive $d\pi-p\pi$ interactions and to obtain the maximum bond order of 2.5 to each oxo.[74] The chloro ligand in $Re^{VI}(O)(ap^{Ph})(isq^{Ph})Cl$ is a poor π base, so population of a π-symmetry d_{xy} orbital does not lead to significant $d\pi-p\pi$ repulsion. Accordingly, the thermodynamic bias for ligand rather than metal oxidation in $Re^{VI}(O)(ap^{Ph})(isq^{Ph})Cl$ is a consequence of the fact that $[Re^{VII}(O)_2(ap^{Ph})_2]^-$ would be significantly destabilized with an electron count other than d^0, but the d^1 electron count is not destabilizing in $Re^{VI}(O)(ap^{Ph})(isq^{Ph})Cl$.

Previously, the capacity of aminophenol- and catechol-derived ligands to supply $1e^-$ in radical-type Re−O bond-forming reactions at $[Re^{V}(O)(ap^{Ph})_2]^-$ and its analogues had been inferred from kinetics studies and computed reaction intermediates,[51,52] but experimental evidence for the intermediacy of ligand radicals was mostly indirect. Isolation of the $Re^{VI}(O)(ap^{Ph})(isq^{Ph})X$ complexes proves that an $[ap^{Ph}]^{2-}$ ligand electron can be utilized for a redox Re−X bond-forming reaction at $[Re^{V}(O)(ap^{Ph})_2]^-$. Gratifyingly, the computational and experimental data are in excellent agreement. In particular, the computed product of O_2 addition to $[Re^{V}(O)(cat)_2]^-$ ($[cat]^{2-}$ = 1,2-catecholate) is a triplet diradical complex, $[Re^{V}(O)(O_2^{\bullet-})(cat)(sq)]^-$ ($[sq]^{\bullet-}$ = 1,2-semiquinonate), containing a partially reduced η^1-superoxide $[O_2^{\bullet}]^-$ ligand and a semiquinonate $[sq]^{\bullet-}$ radical localized to the ligand trans to the oxo group.[51] This reaction is illustrated in Scheme 5a. The addition of a $[Cl]^+$ electrophile to $[Re^{V}(O)(ap^{Ph})_2]^-$ similarly generates a product with one radical ligand (Scheme 5b), and X-ray data for the $Re^{VI}(O)(ap^{Ph})(isq^{Ph})X$ compounds confirm that the $[isq^{Ph}]^{\bullet-}$ ligand radicals are again localized on the ligands trans to the oxo group. This preferred stereochemistry for the C_1-symmetric complexes is likely a function of the strong trans influence of the oxo and the weaker σ basicity of the monoanionic $[sq]^{\bullet-}$ or $[isq^{Ph}]^{\bullet-}$ radicals as compared to the $[cat]^{2-}$ or $[ap^{Ph}]^{2-}$ dianions. This geometric preference can also rationalize the diamagnetism of $Re^{VI}(O)(ap^{Ph})(isq^{Ph})Cl$. When the $Re-O_{oxo}$ bond is coincident with the z axis, $Re^{VI}(O)(ap^{Ph})(isq^{Ph})Cl$ has a d_{xy}^1 configuration. The redox-active $[isq^{Ph}]^{\bullet-}/[ap^{Ph}]^{2-}$ highest occupied molecular orbital has an in-phase combination of N and O p orbitals that can mix with the metal π-symmetry orbitals. However, as shown in Figure 6a, only the ligand that is parallel to the $Re-O_{oxo}$ bond has the correct symmetry to mix with the single occupied d_{xy} orbital. This presumably facilitates antiferromagnetic coupling between the $[isq^{Ph}]^{\bullet-}$ ligand radical and the d^1 metal, leading to the observed $S = 0$ ground state.

Scheme 5

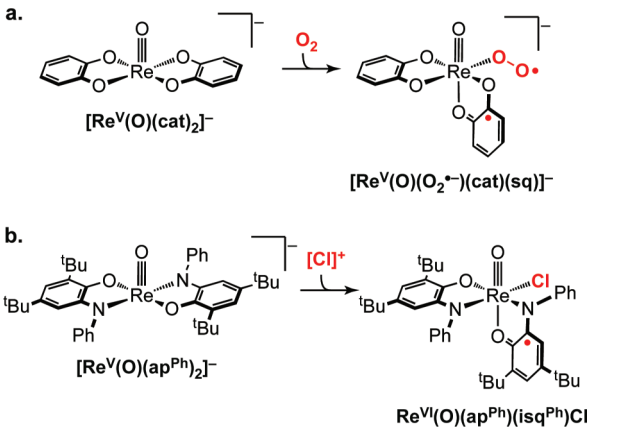

Re−O Bond Formation via Metal-Centered Radical Trapping. The observation of ligand radicals in the $Re^{VI}(O)(ap^{Ph})(isq^{Ph})X$ complexes provides good evidence for the capacity of redox-active $[ap^{Ph}]^{2-}$ ligands to supply electrons in net $2e^-$ redox Re−X bond-forming reactions. However, it does not help to distinguish the preferred site of $1e^-$ oxidation (metal versus ligand) in the kinetic products of O_2 or TEMPO$^\bullet$ radical coupling at $[Re^{V}(O)(ap^{Ph})_2]^-$.[51,52] We therefore pursued the preparation of a monomeric $1e^-$ oxidation product $Re^{V}(O)(ap^{Ph})(isq^{Ph})$ or $[Re^{V}(O)(ap^{Ph})(isq^{Ph})Cl]^-$. However, all attempted syntheses led to the formation of a diamagnetic bis(μ-oxo)dirhenium complex. Electrochemical experiments revealed that the desired $S = {}^1/_2$ monomers are inaccessible because $1e^-$ oxidation of $[Re^{V}(O)(ap^{Ph})_2]^-$ effects rapid dimerization, even in the presence of excess Cl^-. Without X-ray crystallography data of sufficient quality to assign the ligand oxidation states, we tentatively formulate the dimer as $Re^{V}{}_2(\mu\text{-}O)_2(ap^{Ph})_2(isq^{Ph})_2$, implying that the ligands are oxidized. Some support for this assignment comes from isolation of the $S = {}^1/_2$ $Re^{V}(ap^{Ph})(isq^{Ph})Cl_2$ monomer. X-ray data on this complex, which is isoelectronic to $[Re^{V}(O)(ap^{Ph})(isq^{Ph})Cl]^-$, are most consistent with its formulation as a d^2 metal coordinated to a ligand-centered radical.

Because the same bis(μ-oxo) dimer is obtained from $1e^-$ oxidation of $[Re^{V}(O)(ap^{Ph})_2]^-$ or $1e^-$ reduction of $Re^{VI}(O)(ap^{Ph})(isq^{Ph})Cl$ and because Cl^- binding at $[Re^{V}(O)(ap^{Ph})(isq^{Ph})Cl]^-$ is weak, we can infer that both the oxidative and reductive routes to $Re^{V}{}_2(\mu\text{-}O)_2(ap^{Ph})_2(isq^{Ph})_2$ likely proceed through a common five-coordinate $Re^{V}(O)(ap^{Ph})(isq^{Ph})$ intermediate (Scheme 6). However, the comproportionation route to $Re^{V}{}_2(\mu\text{-}O)_2(ap^{Ph})_2(isq^{Ph})_2$ merits further consideration. Scheme 7 shows three possible mechanisms for the net reaction $Re^{V}(O)(ap^{Ph})(isq^{Ph})Cl + [Re^{V}(O)(ap^{Ph})_2]^- \rightarrow Re^{V}{}_2(\mu\text{-}O)_2(ap^{Ph})_2(isq^{Ph})_2 + Cl^-$. Mechanism i of initial Cl^- dissociation, followed by ET, can likely be ruled out because the rate of the comproportionation reaction is apparently unaffected by the addition of excess Cl^- (as 100 equiv of $[Et_4N]Cl$) to the reaction mixture. $Re^{VI}(O)(ap^{Ph})(isq^{Ph})Cl$ is reduced at $E_{pc} = -0.59$ V and $[Re^{V}(O)(ap^{Ph})_2]^-$ is

dx.doi.org/10.1021/ic200923q |Inorg. Chem. 2011, 50, 9864–9878

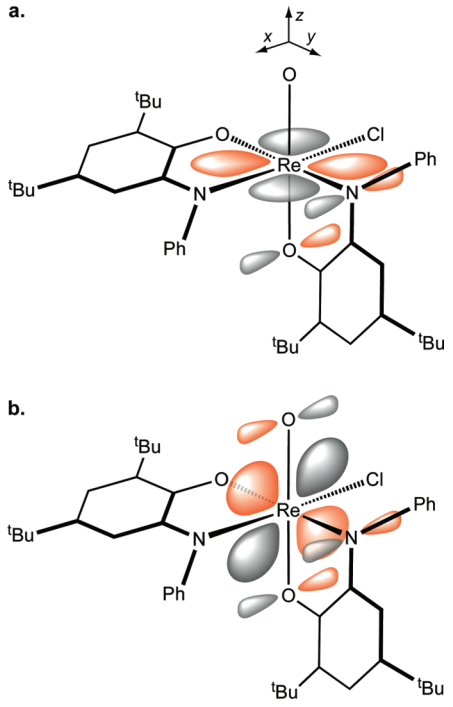

Figure 6. Qualitative π-orbital interactions in $Re^{VI}(O)(ap^{Ph})(isq^{Ph})Cl$.

oxidized at $E_{pa} = -0.35$ V, so initial outer-sphere ET in mechanism ii is thermodynamically uphill, but only by ca. 6 kcal mol^{-1}. Electrochemical and chemical redox experiments demonstrated that the resulting ET products $Re^{V}(O)(ap^{Ph})(isq^{Ph})$ and $[Re^{V}(O)(ap^{Ph})(isq^{Ph})Cl]^{-}$ will rapidly dimerize to $Re^{V}_2(\mu\text{-}O)_2(ap^{Ph})_2(isq^{Ph})_2$, so mechanism ii is consistent with the data available.

Mechanism iii invokes the direct attack of the oxo ligand in $Re^{VI}(O)(ap^{Ph})(isq^{Ph})Cl$ on $[Re^{V}(O)(ap^{Ph})_2]^{-}$ to initially generate an asymmetric μ-oxo dimer, followed by a loss of Cl^{-} and collapse of the dimer to generate the second Re−O bond in $Re^{V}_2(\mu\text{-}O)_2(ap^{Ph})_2(isq^{Ph})_2$. The first step of this proposed mechanism is particularly interesting because it is reminiscent of the redox Re−O bond-forming steps in the reactions of $[Re^{V}(O)(ap^{Ph})_2]^{-}$ with O_2 and nitroxyl radicals.[51,52] For instance, as shown in Scheme 1, we have argued that TEMPO$^{\bullet}$ complexation at $[Re^{V}(O)(cat)_2]^{-}$ likely occurs with $1e^{-}$ transfer to generate a closed-shell $[TEMPO]^{-}$ anion and concomitant oxidation of a $[cat]^{2-}$ ligand to an $[sq]^{\bullet-}$ radical.[52] Scheme 5a shows how forming a new Re−O_2 bond at the oxorhenium(V) center in $[Re^{V}(O)(cat)_2]^{-}$ similarly requires $1e^{-}$ oxidation of a redox-active ligand. Because the formation of $Re^{V}_2(\mu\text{-}O)_2(ap^{Ph})_2(isq^{Ph})_2$ from $Re^{VI}(O)(ap^{Ph})(isq^{Ph})Cl$ and $[Re^{V}(O)(ap^{Ph})_2]^{-}$ generates new Re−O bonds with net $1e^{-}$ transfer, we wondered whether the initial Re−O bond-forming reaction in mechanism iii could be a radical process, analogous to O_2 or nitroxyl radical addition at $[Re^{V}(O)(cat)_2]^{-}$. An intriguing consequence of this proposal is that it suggests that the oxo ligand in $Re^{VI}(O)(ap^{Ph})(isq^{Ph})Cl$ can react like an oxyl radical.

Radical Addition at a Closed-Shell Terminal Oxo Ligand. The capacity of $Re^{VI}(O)(ap^{Ph})(isq^{Ph})Cl$ to undergo radical coupling at the oxo ligand is revealed in its reaction with trityl $Ph_3C^{\bullet}$. As described above, the rhenium-containing products of Scheme 4 are consistent with net oxo transfer from $Re^{VI}(O)(ap^{Ph})(isq^{Ph})Cl$ to $Ph_3C^{\bullet}$. However, the triphenylmethoxyl $Ph_3CO^{\bullet}$ radical does not persist in solution,[87] which suggests

Scheme 6

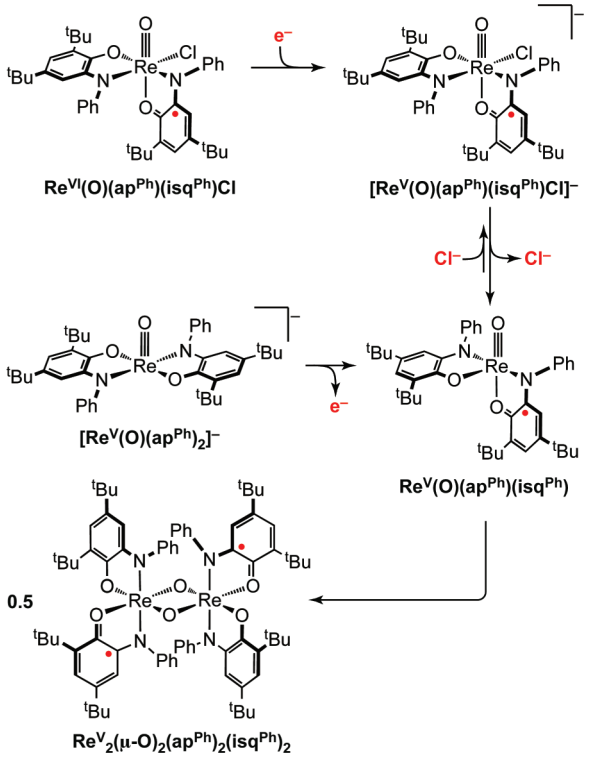

that C−O bond formation occurs at the oxo ligand in $Re^{VI}(O)(ap^{Ph})(isq^{Ph})Cl$. This would generate a triphenylmethoxide complex $Re^{V}(OCPh_3)(ap^{Ph})(isq^{Ph})Cl$ analogous to $Re^{V}(ap^{Ph})(isq^{Ph})Cl_2$. Two mechanisms for formation of the putative alkoxide complex are shown in Scheme 8. Initial outer-sphere ET (mechanism i) is unlikely because the reduced rhenium product $[Re^{V}(O)(ap^{Ph})(isq^{Ph})Cl]^{-}$ is known to rapidly form the bis(μ-oxo) dimer $Re^{V}_2(\mu\text{-}O)_2(ap^{Ph})_2(isq^{Ph})_2$, which is inert to Ph_3C^{+}. Mechanism ii of direct $Ph_3C^{\bullet}$ addition to $Re^{VI}(O)(ap^{Ph})(isq^{Ph})Cl$ is more reasonable. Metal oxo complexes are known to add carbon radicals to make C−O bonds.[68,88,89] For example, alkoxide complexes are obtained by R$^{\bullet}$ radical addition to $Cr(O)_2Cl_2$,[68,90,91] and oxidations of triphenylmethane Ph_3CH that occur by a rebound mechanism presumably generate the C−O bond in Ph_3COH by trapping $Ph_3C^{\bullet}$ at a M−OH transient.[88,92−94] Accordingly, although trityl oxidation at metal oxos is, to our knowledge, rarely reported, the reaction is probably not unprecedented. The formation of Ph_3COH from the putative $Re^{V}(OCPh_3)(ap^{Ph})(isq^{Ph})Cl$ complex intermediate requires 1 equiv of H$^{\bullet}$, but added reductants were not needed to observe Ph_3COH. In the absence of any observable $Re^{V}(OCPh_3)(ap^{Ph})(isq^{Ph})Cl$, we speculate that steric pressure in $Re^{V}(OCPh_3)(ap^{Ph})(isq^{Ph})Cl$ may weaken the Re−OR bond, facilitating the generation of Ph_3COH by reaction with adventitious reductant.

Although Mayer and co-workers have convincingly argued that unpaired spin density at oxygen is not a prerequisite for radical R$^{\bullet}$ addition at a terminal oxo group,[68,70] recent reports continue to suggest that complexes with ligand free radicals,[95−98] including metal oxyls,[55−59,62−67] are active for radical bond-making and -breaking reactions at the terminal ligand. In this context, $Re^{VI}(O)(ap^{Ph})(isq^{Ph})Cl$ is an unusual radical scavenger because it is neither a strong oxidant nor a ground-state oxyl radical. As described above,

dx.doi.org/10.1021/ic200923q |*Inorg. Chem.* 2011, 50, 9864–9878

Scheme 7

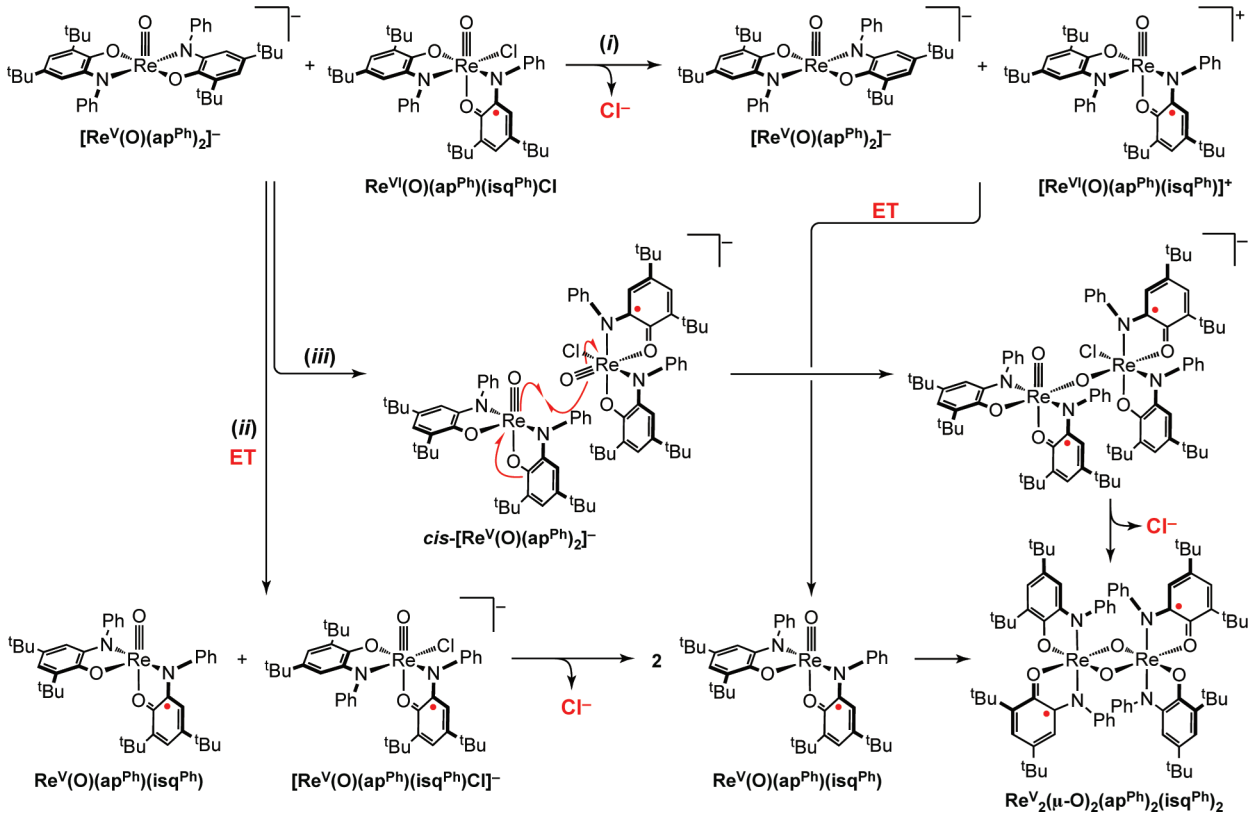

Scheme 8

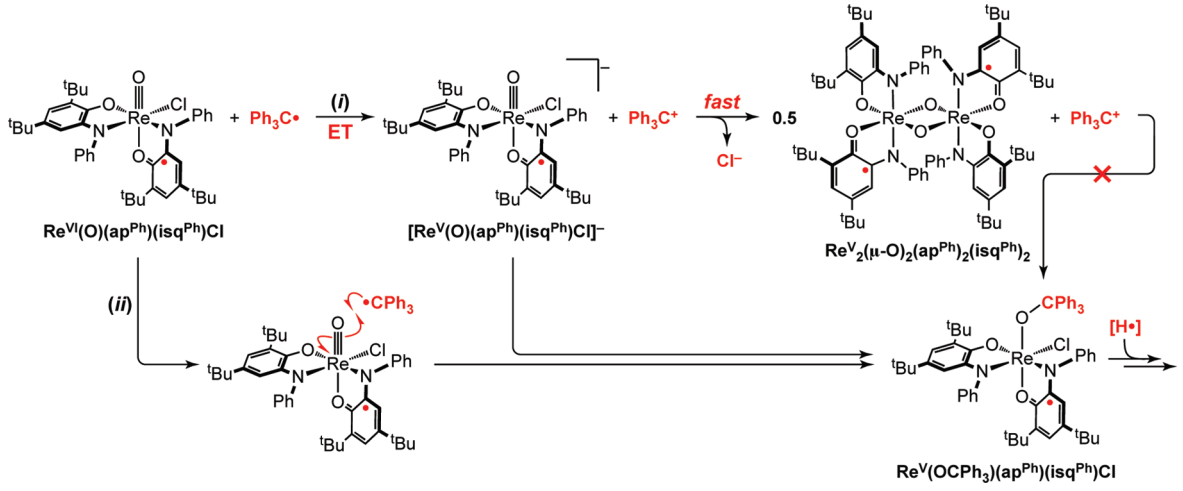

$Re^{VI}(O)(ap^{Ph})(isq^{Ph})Cl$ is ca. 550 mV less oxidizing than ferrocenium. $Re^{VI}(O)(ap^{Ph})(isq^{Ph})Cl$ is not a strong oxo donor, as evidenced by its inability to oxidize PPh_3 under conditions analogous to those for $Ph_3C^•$ oxidation.[85,86] Moreover, none of the related $Re^{V}_2(\mu\text{-}O)_2(ap^{Ph})_2(isq^{Ph})_2$, $[Re^{V}(O)(ap^{Ph})_2]^-$, and $[Re^{VII}(O)_2(ap^{Ph})_2]^-$ complexes show any propensity to make a C−O bond to the $[Ph_3C]$ fragment (as $Ph_3C^•$ or Ph_3C^+). The contrast with $[Re^{VII}(O)_2(ap^{Ph})_2]^-$ is particularly notable; the addition of PPh_3 to $[Re^{VII}(O)_2(ap^{Ph})_2]^-$ generates $[Re^{V}(O)(ap^{Ph})_2]^-$ and $OPPh_3$ in seconds.[51] This suggests that the differences in oxo transfer to $Ph_3C^•$ must derive from kinetic and not thermodynamic factors.

Generation of an oxyl radical typically requires single-electron occupancy of a metal−oxo π^*-symmetry antibonding orbital.[63,68,74] The metal-based unpaired electron in $Re^{VI}(O)(ap^{Ph})(isq^{Ph})Cl$ does not satisfy this criterion because it is in a d_{xy} orbital orthogonal to the $Re-O_{oxo}$ π-bonding manifold (Figure 6a). However, another approach to oxyl radical formation is to remove an electron from a metal−oxo π-bonding orbital. Because these bonding orbitals are typically low in

dx.doi.org/10.1021/ic200923q |Inorg. Chem. 2011, 50, 9864–9878

energy,[74] this approach is usually energetically prohibitive. Notably, the $[isq^{Ph}]^{\bullet-}$ ligand trans to the oxo has its unpaired electron in a π-symmetry orbital that overlaps with d_{xy} as well as one of the two $d_{xy/yz}$ orbitals that are used to form the Re≡O π bonds (Figure 6b). Accordingly, symmetry-allowed mixing of the $[isq^{Ph}]^{\bullet-}$ ligand with a Re≡O π bond delocalizes the $[isq^{Ph}]^{\bullet-}$ hole into the $Re-O_{oxo}$ π system. In the limit of strong intraligand CT $[O]^{2-} \rightarrow [isq^{Ph}]^{\bullet-}$, the $Re-O_{oxo}$ bond order decreases from 3.0 to 2.5 and the complex is an oxyl radical. However, the oxidation potentials for $[ap^{Ph}]^{2-}$ and $[O]^{2-}$ imply that $[O]^{2-} \rightarrow [isq^{Ph}]^{\bullet-}$ ET is a high-energy process, so it is not appropriate to describe the ground-state electronic structure of $Re^{VI}(O)(ap^{Ph})(isq^{Ph})Cl$ as $Re^{VI}(O^{\bullet})(ap^{Ph})_2Cl$ with a true oxyl radical. However, it is not unreasonable to expect that mixing of the $[isq^{Ph}]^{\bullet-}$ singly occupied molecular orbital with a Re≡O π bond may give oxyl radical character to the oxo ligand in $Re^{VI}(O)(ap^{Ph})(isq^{Ph})Cl$ and that this may impact the capacity of the closed-shell oxo ligand to undergo radical bond-forming redox reactions.

FUTURE DIRECTIONS

Using Redox-Active Ligands for Oxyl Radical Reactions. All of the five-coordinate redox-active ligand oxorhenium complexes described in this study have a demonstrated propensity to undergo radical addition at the rhenium center, but the discovery of trityl radical addition at oxo is unique to $Re^{VI}(O)(ap^{Ph})(isq^{Ph})Cl$. We ascribe this bias for ligand-centered coupling in $Re^{VI}(O)(ap^{Ph})(isq^{Ph})Cl$ to the coordinatively saturated and sterically congested rhenium center, which directs radical addition away from the metal. Radical addition at a terminal oxo group does not necessarily implicate unpaired spin density at the oxo ligand, but it is noteworthy that all of the closed-shell oxorhenium homologues are inert to $Ph_3C^{\bullet}$, including some that have a demonstrated efficacy for oxo transfer to other substrates. Accordingly, if radical density at oxygen is important for this reaction, additional geometrical and electronic constraints are probably critical. First, the redox-active ligand radical should be localized in a site that is not itself prone to odd-electron reactions. Second, we propose that symmetry-allowed mixing of the ligand radical with the metal oxo π-bonding manifold is crucial for redox-active ligand-mediated oxyl reactivity. The $Re^{VI}(O)(ap^{Ph})(isq^{Ph})X$ complexes meet all of these criteria, but the design principles are general and transferrable. This hypothesis is therefore testable using a variety of metals, redox-active ligands, and coordination complex geometries. It is also clear that this approach will benefit greatly from recently developed computational methods to analyze the electronic structures of complexes containing strongly interacting open-shell metals and redox-active ligands.

Harnessing intraligand CT for radical reactions at closed-shell oxo ligands represents a new way to utilize redox-active ligands for small-molecule activation and functionalization. Unpaired spin at oxygen may not be a prerequisite for radical $R^{\bullet}$ addition at a terminal oxo group, but it is not clear whether radical coupling at oxyls would be more kinetically facile than $R^{\bullet}$ addition to closed-shell oxos, given the same thermodynamic driving force. Accordingly, this strategy holds exciting implications for the design of kinetically reactive oxidants that utilize low-barrier radical redox steps in selective multielectron redox transformations. The experiments described herein represent our first efforts in this regard. Attempts to extend this approach to other redox-active ligand metal oxo complexes, and to delineate the effects of unpaired spin in radical addition at oxo ligands, are ongoing.

EXPERIMENTAL DETAILS

General Considerations. Unless otherwise specified, all manipulations were performed under anaerobic conditions using standard vacuum-line techniques or in an inert-atmosphere glovebox under purified nitrogen. Routine NMR spectra were acquired on a Varian Mercury 300 spectrometer (300.323 MHz for ^1H) at ambient temperature. Variable-temperature and two-dimensional NMR spectra were obtained with a Bruker AMX 400 spectrometer (400.138 MHz for ^1H). Chemical shifts are reported in parts per million (ppm) relative to tetramethylsilane, with the residual solvent peak serving as an internal reference. Solution-state magnetic moments were determined by Evans' NMR method.[75,76] Solid-state magnetism data were recorded using a Quantum Design MPMS-5S SQUID magnetometer. Samples were analyzed using 5−10 mg of powdered material loaded into a 0.5 mm × 1.5 mm gelatin capsule, wrapped in Kapton tape, and inserted into a plastic straw. Data were obtained using a 100 G field between 5 and 400 K. UV−visible absorption spectra were acquired using a Varian Cary 50 spectrophotometer. Unless otherwise specified, all electronic absorption spectra were recorded at 25 °C in 1 cm quartz cells. IR spectra were obtained by attenuated total reflectance (ATR) through a diamond plate on a Bruker Optics Alpha-P Fourier transform infrared (FTIR) spectrometer. All mass spectra were recorded at the Georgia Institute of Technology Bioanalytical Mass Spectrometry Facility. Matrix-assisted laser desorption/ionization mass spectrometry (MALDI-MS) was obtained using an Applied Biosystems 4700 proteomics analyzer. Gas chromatography−mass spectrometry (GC−MS) analyses used an Agilent 6890 gas chromatograph equipped with an autosampler and a Restek Rxi-5 ms column (30 m × 0.25 mm i.d., 0.25 μm film thickness). Injections of 1 μL were made at a 50:1 split ratio. The GC oven program consisted of a hold at 30 °C for 1 min, followed by a 15 °C min^{-1} ramp to 300 °C, and then a hold at 300 °C for 11 min. The mass spectrometer used in tandem was a Micromass AutoSpec electronionization (EI) detector. For GC−MS quantitation of organics, *n*-decane (1 μL) was added to serve as an internal standard and product yields were determined by a comparison of the EI-MS detector responses against calibration curves derived from the pure materials, as well as by a comparison to the detector response for *n*-decane. Cyclic voltammetric measurements were made using a CH Instruments CHI620C potentiostat in a three-component cell consisting of a platinum disk working electrode, a platinum wire auxiliary electrode, and a nonaqueous $AgPF_6/Ag$ reference electrode. Electrochemical data are referenced and reported to Fc^+/Fc as an internal standard. Elemental analyses were performed by Atlantic Microlab, Inc., Norcross, GA. All analyses were performed in duplicate, and the reported compositions are the average of the two runs.

Methods and Materials. Anhydrous acetonitrile (CH_3CN), dichloromethane (CH_2Cl_2), and tetrahydrofuran (THF) solvents for air- and moisture-sensitive manipulations were purchased from Sigma-Aldrich and further dried by passage through columns of activated alumina, degassed by at least three freeze−pump−thaw cycles, and stored under N_2 prior to use. Benzene was purchased from Sigma-Aldrich, degassed by three freeze−pump−thaw cycles, vacuum distilled from CaH_2, and stored under dry N_2. Methanol (anhydrous, 99.0%) was purchased from Honeywell Burdick and Jackson. Acetone (99.8%, extra dry) was purchased from Acros. Both were used as received. Deuterated acetonitrile (CD_3CN) and dichloromethane (CD_2Cl_2) were purchased from Cambridge Isotope Laboratories, degassed by three freeze−pump−thaw cycles, vacuum distilled from CaH_2, and stored under a dry N_2 atmosphere prior to use. $(Et_4N)[Re^{V}(O)(ap^{Ph})_2]$,[51] $(Et_4N)[Re^{VII}(O)_2(ap^{Ph})_2]$,[51] $[Ph_3C][BF_4]$,[99] and triphenylmethyl radical $Ph_3C^{\bullet}$ dimer[100] in C_6H_6 were prepared by literature methods. All characterization data matched those referenced. All other reagents were purchased from Sigma-Aldrich and used as received.

Synthesis of $Re^{VI}(O)(ap^{Ph})(isq^{Ph})(OC_6Cl_5)$. A 150 mL flask with a Kontes brand high-vacuum poly(tetrafluoroethylene) (PTFE) valve

dx.doi.org/10.1021/ic200923q |*Inorg. Chem.* 2011, 50, 9864–9878

was charged with $(Et_4N)[Re^{V}(O)(ap^{Ph})_2]$ (568 mg, 0.616 mmol) and dissolved in THF (40 mL). Separately, 2,3,4,5,6,6-hexachloro-2,4-cyclohexadien-1-one (222 mg, 0.742 mmol) was dissolved in THF (3 mL) and added to the $[Re^{V}(O)(ap^{Ph})_2]^{-}$ solution, giving an immediate color change from pale green to dark purple. The reaction mixture was stirred at 60 °C for 10 days under N_2. The mixture was then exposed to air and the solvent removed in vacuo. The dark residue was taken up in minimal CH_2Cl_2 and chromatographed on a silica gel column (230−400 mesh) prepared with hexanes. A dark-purple band eluted as the second, major fraction using 70:30 hexanes/CH_2Cl_2. Removal of the solvent from the eluate, followed by dissolution in benzene and lyophilization, afforded analytically pure $Re^{VI}(O)(ap^{Ph})(isq^{Ph})(OC_6Cl_5)$ (364 mg, 0.345 mmol, 71%) as a purple powder. Single crystals for X-ray diffraction analysis were grown by the slow evaporation of a saturated CH_3CN solution at 8 °C over 2 weeks on a Chromel A (80% Ni and 20% Cr) wire. UV−vis (CH_3CN) λ_{max}, nm (ε, M^{-1} cm^{-1}): 231 (50 000), 413 (13 300), 523 (17 100), 613 (sh), 894 (3500). MALDI-MS (m/z): 1058 $[M]^+$. FTIR (ATR, cm^{-1}): 2953 (m), 2923 (m), 2866 (m), 1590 (vw), 1532 (vw), 1479 (m), 1458 (m), 1386 (vs), 1359 (s), 1313 (vw), 1299 (vw), 1252 (m), 1225 (w), 1203 (w),1164 (w), 1135 (w), 1108 (w), 1077 (w), 1027 (w), 989 (s), 934 (s), 924 (s), 894 (w), 880 (w), 864 (w), 830 (vs), 778 (s), 711 (s), 674 (vs), 608 (vw), 553 (s), 426 (m). ^{1}H NMR (300 MHz, CD_2Cl_2, δ): 7.7 (td, J = 7 and 2 Hz, N*Ph*: meta, 1H), 7.64 (d, J = 7 Hz, N*Ph*: ortho, 1H), 7.63 (td, J = 7 and 2 Hz, N*Ph*: meta, 1H), 7.44 (tt, J = 7 Hz, 1 Hz, N*Ph*: para, 1H), 7.32 (t, J = 7 Hz, N*Ph′*: meta, 1H), 7.18 (d, J = 7 Hz, N*Ph′*: ortho, 1H), 7.08 (d, J = 7 Hz, N*Ph*: ortho, 1H), 6.98 (d, J = 2 Hz, Ar*H*, 1H), 6.97 (t, J = 7 Hz, N*Ph′*: meta, 1 H), 6.95 (t, J = 7 Hz, N*Ph′*: para, 1H), 6.59 (d, J = 2 Hz, Ar*H*, 1H), 6.53 (d, J = 2 Hz, Ar*H*, 1H), 6.51 (d, J = 2 Hz, Ar*H*, 1H), 6.00 (d, J = 7 Hz, N*Ph′*: ortho, 1H), 1.23 (s, ^{t}Bu, 9H), 1.19 (s, ^{t}Bu, 9H), 1.17 (s, ^{t}Bu, 9H), 0.98 (s, br, ^{t}Bu, 9H). The reported analysis is for $Re^{VI}(O)(ap^{Ph})(isq^{Ph})(OC_6Cl_5)\cdot C_6H_6$, and the presence of 1 equiv of benzene in the sample was confirmed by ^{1}H NMR spectroscopy. Anal. Calcd for $C_{53}H_{64}Cl_5N_2O_4Re$: C, 55.04; H, 5.58; N, 2.42. Found: C, 55.19; H, 5.22; N, 2.40.

Synthesis of $Re^{VI}(O)(ap^{Ph})(isq^{Ph})Cl$. Method 1. The procedure above for the synthesis of $Re^{VI}(O)(ap^{Ph})(isq^{Ph})(OC_6Cl_5)$ yields $Re^{VI}(O)(ap^{Ph})(isq^{Ph})Cl$ (62 mg, 0.075 mmol, 12%) as a minor product. **Method 2.** A 20 dram scintillation vial was charged with $(Et_4N)[Re^{V}(O)(ap^{Ph})_2]$ (25.9 mg, 0.0281 mmol) and dissolved in CH_3CN (5 mL) to afford a pale-green solution. A second 20 dram scintillation vial was charged with tris(4-bromophenyl)ammoniumyl hexachloroantimonate $[(C_6H_4Br)_3N][SbCl_6]$ (25.8 mg, 0.0316 mmol) and dissolved in CH_3CN (2 mL). Both solutions were chilled to −20 °C and combined to immediately yield a dark-purple solution. The reaction mixture was stored at −20 °C for 6 months to deposit purple crystals of $Re^{VI}(O)(ap^{Ph})(isq^{Ph})Cl$ (2.7 mg, 3.26 mmol, 11%) that were used for X-ray diffraction analysis. **Method 3.** A 20 dram scintillation vial was charged with $Re^{VI}(O)(ap^{Ph})(isq^{Ph})(OC_6Cl_5)$ (30.0 mg, 0.0284 mmol) and dissolved in 1:1 CH_2Cl_2/CH_3CN (10 mL) in air. Excess concentrated aqueous HCl (200−300 μL; 2.48−3.72 mmol) was added dropwise, and the reaction mixture was stirred at ambient temperature for 15 h in air. The reaction mixture was washed with water (3 × 5 mL) to remove unreacted HCl, and the organic layer was separated and dried on $MgSO_4$. Filtration followed by removal of the solvent under reduced pressure gave purple solids of $Re^{VI}(O)(ap^{Ph})(isq^{Ph})Cl$ in quantitative isolated yield. UV−vis (CH_2Cl_2) λ_{max}, nm (ε, M^{-1} cm^{-1}): 295 (sh), 410 (10 500), 515 (12 300), 605 (sh), 920 (1700). MALDI-MS (m/z): 828 $[M]^+$. FTIR (ATR, cm^{-1}): 2958 (m), 2905 (m), 2868 (m), 1588 (m), 1532 (m), 1481 (s), 1451 (m), 1407 (w), 1391 (m), 1362 (s), 1320 (m), 1302 (m), 1264 (s), 1250 (s), 1176 (s), 1111 (w), 1070 (w), 1027 (m), 995 (s), 928 (vs), 915 (vs), 859 (s), 834 (m), 772 (m), 758 (m), 741 (w), 714 (vs), 703 (vs), 671 (m), 652 (m), 643 (s), 616 (s), 555 (m), 541 (m), 503 (m), 474 (w). ^{1}H NMR (293 K, 400 MHz, CD_2Cl_2, δ): 7.63 (td, J = 7 and 2 Hz, N*Ph*: meta, 1H), 7.54 (td, J = 7 and 2 Hz, N*Ph*: meta, 1H), 7.45 (d, J = 7 Hz, N*Ph*: ortho, 1H), 7.40 (tt, J = 7 and 1 Hz, N*Ph*: para, 1H), 7.2 (t, J = 7 Hz, N*Ph′*: meta, 2H), 6.97 (tt, J = 7 and 1 Hz, N*Ph′*: ortho, para, 2H), 6.93 (d, J = 2 Hz, Ar*H*, 1H), 6.66 (d, J = 7 Hz, N*Ph*: ortho, 1H), 6.52 (d, J = 2 Hz, Ar*H*, 1H), 6.4 (d, J = 2 Hz, Ar*H*, 1H), 6.29 (br, N*Ph′*: ortho, 1H), 6.26 (d, J = 2.1 Hz, Ar*H*, 1H), 1.48 (s, ^{t}Bu Hz, 9H), 1.22 (s, ^{t}Bu Hz, 9H), 1.20 (s, ^{t}Bu, 9H), 1.18 (s, ^{t}Bu, 9 H). ^{1}H NMR (253 K, 400 MHz, CD_2Cl_2, δ): 7.63 (t, J = 7 Hz, N*Ph*: meta, 1H), 7.56 (t, J = 7 Hz, N*Ph*: meta, 1H), 7.44 (d, J = 7 Hz, N*Ph*: ortho, 1H), 7.41 (t, J = 7 Hz, N*Ph*: para, 1H), 7.24 (t, J = 7 Hz, N*Ph′*: meta, 1H), 7.17 (t, J = 7 Hz, N*Ph′*: meta, 1H), 7.01 (d, J = 7 Hz, N*Ph′*: ortho 1H), 6.96 (t, J = 7 Hz, N*Ph′*: para, 1H), 6.92 (d, J = 2 Hz, Ar*H*, 1H), 6.75 (d, J = 7 Hz, N*Ph*: ortho 1H), 6.47 (d, J = 2 Hz, Ar*H*: 1H), 6.40 (d, J = 2 Hz, Ar*H*, 1H), 6.33 (d, J = 7 Hz, N*Ph′*: ortho, 1H), 6.28 (d, J = 2 Hz, Ar*H*, 1H), 1.44 (s, ^{t}Bu, 9H), 1.17 (s, ^{t}Bu, 18H), 1.15 (s, ^{t}Bu, 9H). Samples for combustion analysis were prepared by method 3, above, which produces pentachlorophenol as a byproduct. The reported analysis is for $Re^{VI}(O)(ap^{Ph})(isq^{Ph})Cl\cdot 0.5C_6H_6\cdot 0.8C_6Cl_5OH$. The presence of benzene in the sample was confirmed by ^{1}H NMR spectroscopy. Anal. Calcd for $C_{47.8}H_{53.8}Cl_5N_2O_{3.8}Re$: C, 53.13; H, 5.02; N, 2.59. Found: C, 53.06; H, 5.15; N, 2.70.

Synthesis of $Re^{V}_2(\mu\text{-}O)_2(ap^{Ph})_2(isq^{Ph})_2$. Method 1. In a 20 mL scintillation vial, a solution of $Re^{VI}(O)(ap^{Ph})(isq^{Ph})Cl$ (25.6 mg, 0.031 mmol) in CH_2Cl_2 (5 mL) was added to a solution of bis(benzene)-chromium $[Cr(|^6\text{-}C_6H_6)_2]$ (6.3 mg, 0.031 mmol) in CH_2Cl_2 (5 mL) to yield a purple solution. The reaction mixture was stirred for 20 min, and the solvent was removed under vacuum. The resulting purple residue was extracted into ether and the solvent removed in vacuo to afford $Re^{V}_2(\mu\text{-}O)_2(ap^{Ph})_2(isq^{Ph})_2$ (19.3 mg, 0.0120 mmol, 79%) as a purple powder. Recrystallization by the slow evaporation of a concentrated CH_2Cl_2 solution afforded single crystals suitable for X-ray diffraction analysis. **Method 2.** A 20 dram scintillation vial was charged with $(Et_4N)[Re^{V}(O)(ap^{Ph})_2]$ (0.327 g, 0.355 mmol) and dissolved in CH_3CN (10 mL) to afford a pale-green solution. The addition of tris(4-bromophenyl)ammoniumyl tetrafluoroborate $[(C_6H_4Br)_3N][BF_4]$ (0.1963 g, 0.345 mmol) in MeCN (5 mL) with vigorous stirring gave the immediate formation of a dark precipitate. After stirring for 30 min, the solids were collected by vacuum filtration to give $Re^{V}_2(\mu\text{-}O)_2(ap^{Ph})_2(isq^{Ph})_2$ (0.532 g, 0.335 mmol, 97%) as a dark-purple powder. Single crystals of $Re^{V}_2(\mu\text{-}O)_2(ap^{Ph})_2(isq^{Ph})_2$ for X-ray diffraction were grown by vapor diffusion of CH_3CN into a concentrated CH_2Cl_2. **Method 3.** A solution of $(Et_4N)[Re^{V}(O)(ap^{Ph})_2]$ (10.7 mg, 0.012 mmol) in CH_2Cl_2 (5 mL) was added to a solution of $Re^{VI}(O)(ap^{Ph})(isq^{Ph})Cl$ (8.9 mg, 0.010 mmol) in CH_2Cl_2 (5 mL), and the reaction mixture was stirred for 10 min. Removal of the solvent gave a purple residue that was extracted into ether and dried in vacuo to yield $Re^{V}_2(\mu\text{-}O)_2(ap^{Ph})_2(isq^{Ph})_2$ (15.2 mg, 0.0096 mmol, 96%) as a dark-purple powder. Single crystals for study by X-ray diffraction were obtained by the slow evaporation of a benzene solution. MALDI-MS (m/z): 1586 $[M]^+$. FTIR (ATR, cm^{-1}): 2953 (s), 2902 (m), 2865 (m), 1589 (m), 1484 (s), 1463 (m), 1391 (m), 1361 (s), 1247 (vs), 1201 (m), 1163 (m), 1024 (m), 994 (s), 928 (m), 888 (s), 861 (s), 832 (s), 765 (s), 708 (vs), 687 (w), 645 (vs), 621 (s), 570 (s), 545 (m), 502 (m), 483 (s), 400 (m). ^{1}H NMR (300 MHz, C_6D_6, δ): 6.8−7.0 (m, Ar, 28H), 1.27 (s, ^{t}Bu, 36 H), 1.1 (s, ^{t}Bu, 36 H). UV−vis (CH_2Cl_2) λ_{max}, nm (ε, M^{-1} cm^{-1}): 300 (sh), 420 (sh), 480 (33 000), 610 (22 700). Anal. Calcd for $C_{80}H_{100}N_4O_4Re_2$: C, 60.58; H, 6.35; N, 3.53. Found: C, 60.03; H, 6.35; N, 3.44.

Synthesis of $Re^{V}(ap^{Ph})(isq^{Ph})Cl_2$. Method 1. A 50 mL flask with a Kontes brand high-vacuum PTFE valve was charged with $(Et_4N)[Re^{V}(O)(ap^{Ph})_2]$ (0.484 g, 0.524 mmol) and CH_2Cl_2 (25 mL). The addition of Me_3SiCl (160 μL, 1.26 mmol) afforded a red-orange solution. The flask was sealed and immersed in a silicone fluid bath at 65 °C for 3 h to yield a clear, maroon solution and then cooled to ambient temperature. The mixture was exposed to air, and the solvent was removed under reduced pressure. The residue was taken up in

dx.doi.org/10.1021/ic200923q |*Inorg. Chem.* 2011, 50, 9864–9878

minimal CH_2Cl_2 (2 mL) and chromatographed on a silica gel column (230−400 mesh) prepared with hexanes. A dark-maroon band eluted as the major, first fraction using CH_2Cl_2. Removal of the solvent from the eluate afforded $Re^{V}(ap^{Ph})(isq^{Ph})Cl_2$ (0.399 g, 0.471 mmol, 90%) as a maroon powder. Single crystals suitable for analysis by X-ray diffraction were obtained by the slow evaporation of a concentrated CH_2Cl_2 solution. **Method 2.** In a 20 dram scintillation vial, a solution of $(Et_4N)[Re^{VII}(O)_2(ap^{Ph})_2]$ (33.4 mg, 0.036 mmol) in CH_2Cl_2 (10 mL) was combined with concentrated aqueous HCl (5 mL, 62 mmol). The reaction mixture was stirred vigorously at ambient temperature for 24 h, during which time the color changed from dark purple to maroon. The reaction mixture was washed with water (3 × 5 mL) to remove unreacted HCl, and the organic layer was separated and dried on $MgSO_4$. Filtration followed by removal of the solvent under reduced pressure gave $Re^{V}(ap^{Ph})(isq^{Ph})Cl_2$ (19.2 mg, 0.023 mmol, 63%) as a maroon powder. UV−vis (CH_2Cl_2) λ_{max}, nm (ε, M^{-1} cm^{-1}): 264 (18 800), 385 (8100), 490 (29 300). MALDI-MS (m/z): 847 $[M]^+$. FTIR (ATR, cm^{-1}): 2951 (s), 2904 (m), 2865 (m), 1585 (m), 1540 (m), 1485 (vs), 1454 (vs), 1393 (w), 1361 (vs), 1305 (w), 1251 (vs), 1231 (m), 1199 (m), 1164 (m), 1109 (w), 1074 (w), 1025 (m), 997 (m), 912 (m), 864 (m), 828 (w), 768 (vs), 735 (vs), 706 (vs), 651 (m), 604 (m), 543 (m), 497 (s), 399 (m). Anal. Calcd for $C_{40}H_{50}Cl_2N_2O_2Re$: C, 56.66; H, 5.94; N, 3.30. Found: C, 56.52; H, 6.28; N, 3.27.

Reactions with the Triphenylmethyl Radical. In a representative procedure, a 20-dram vial was charged with $Re^{VI}(O)(ap^{Ph})(isq^{Ph})Cl$ (78.5 mg, 0.095 mmol) and C_6H_6 (10 mL) was added to create a clear purple solution. A 0.0725 M solution of the triphenylmethyl radical $Ph_3C^{\bullet}$ dimer in C_6H_6 (700 μL, 0.102 mmol $Ph_3C^{\bullet}$) was added. The vial was wrapped in aluminum foil to inhibit disproportionation, and the reaction mixture was stirred for 1 week at ambient temperature. A 1 mL aliquot of the reaction solution was transferred to a 2 mL GC autosampler vial and analyzed by GC−MS to determine the organic product distribution and quantitate Ph_3COH (0.066 mmol, 69% based on initial [Re]). The remaining reaction mixture was dried in vacuo, and the dark residue was washed with MeCN (3 × 5 mL) to give a red-purple solution and a dark precipitate of $Re^{V}_2(\mu\text{-}O)_2(ap^{Ph})_2(isq^{Ph})_2$ (28.5 mg, 0.018 mmol), which was collected by vacuum filtration. The red-purple filtrate was chromatographed on a silica gel column (230−400 mesh) prepared with hexanes. A dark-purple band eluted as the first fraction using 70:30 CH_2Cl_2/hexanes. Removal of the solvent from the eluate followed by dissolution in C_6H_6 and lyophilization gave $Re^{VI}(O)(ap^{Ph})(isq^{Ph})Cl$ (22.9 mg, 0.028 mmol). A maroon band eluted as the second fraction using CH_2Cl_2. Solvent removal from the eluate under reduced pressure gave a dark-maroon powder of $Re^{V}(ap^{Ph})(isq^{Ph})Cl_2$ (22.9 mg, 0.027 mmol).

X-ray Crystallography. Crystals of $Re^{VI}(O)(ap^{Ph})(isq^{Ph})(OC_6Cl_5)\cdot CH_3CN$, $Re^{VI}(O)(ap^{Ph})(isq^{Ph})Cl$, $Re^{V}(ap^{Ph})(isq^{Ph})Cl_2\cdot 0.65CH_2Cl_2$, and $Re^{V}_2(\mu\text{-}O)_2(ap^{Ph})_2(isq^{Ph})_2$ suitable for X-ray diffraction analysis were coated with Paratone N oil, suspended on a small fiber loop, and placed in a cooled nitrogen gas stream at 173 K on a Bruker D8 APEX II CCD sealed-tube diffractometer. Data were collected using graphite-monochromated Mo Kα (λ = 0.710 73 Å) radiation. Data were measured using a series of combinations of ϕ and ω scans with 10 s frame exposures and 0.5° frame widths. Data collection, indexing, and initial cell refinements were all carried out using APEX II software.[101] Frame integration and final cell refinements were done using *SAINT* software.[102] The structures were solved using direct methods and difference Fourier techniques using the *SHELXTL* program package, V6.12.[103] Hydrogen atoms were placed in their expected chemical positions using the HFIX command and were included in the final cycles of least squares with isotropic U_{ij}'s related to the atoms ridden upon. All non-hydrogen atoms in were refined anisotropically except for C2S in $Re^{V}(ap^{Ph})(isq^{Ph})Cl_2\cdot 0.66CH_2Cl_2$, C19, and C24 and the N and O atoms in $Re^{V}_2(\mu\text{-}O)_2(ap^{Ph})_2(isq^{Ph})_2$. Scattering factors and anomalous dispersion corrections are taken from the *International Tables for X-ray Crystallography*.[104] Other details of data collection and structure refinement are provided in Table S1 in the Supporting Information.

■ ASSOCIATED CONTENT

Supporting Information. Tabulated X-ray crystallographic data and structure parameters for $Re^{VI}(O)(ap^{Ph})(isq^{Ph})(OC_6Cl_5)\cdot CH_3CN$, $Re^{VI}(O)(ap^{Ph})(isq^{Ph})Cl$, $Re^{V}_2(\mu\text{-}O)_2(ap^{Ph})_2(isq^{Ph})_2$, and $Re^{V}(ap^{Ph})(isq^{Ph})Cl_2\cdot 0.65CH_2Cl_2$, GC−MS data from a reaction of $Re^{VI}(O)(ap^{Ph})(isq^{Ph})Cl$ with $Ph_3C^{\bullet}$, EI-MS spectra, and X-ray crystallographic information in CIF format. This material is available free of charge via the Internet at http://pubs.acs.org.

■ AUTHOR INFORMATION

Corresponding Author
*E-mail: jake.soper@chemistry.gatech.edu.

■ ACKNOWLEDGMENT

We gratefully acknowledge financial support from a DARPA Young Faculty Award (Grant N6600 1-09-1-2094) and the Georgia Institute of Technology. We thank Dr. Les Gelbaum for assistance with NMR spectroscopy, David Bostwick for mass spectrometry, and Dan Sabo for SQUID magnetometry.

■ REFERENCES

(1) Sheldon, R. A.; Kochi, J. K. *Metal-Catalyzed Oxidations of Organic Compounds*; Academic Press: New York, 1981.
(2) Oxidation. In *Comprehensive Organic Synthesis: Selectivity, Strategy and Efficiency in Modern Organic Chemistry*; Trost, B. M., Fleming, I., Eds.; Pergamon: Oxford, U.K., 1991; Vol. 7.
(3) Cavani, F.; Ballarini, N.; Luciani, S. *Top. Catal.* **2009**, *52*, 935–947.
(4) *Basic Research Needs for Solar Energy Utilization*; U.S. Department of Energy Report of the Basic Energy Sciences Workshop on Solar Energy Utilization, 2005.
(5) *Organic Syntheses by Oxidation with Metal Compounds*; Mijs, W. J., De Jonge, C. R. H. I., Eds.; Plenum Press: New York, 1986.
(6) Parshall, G. W.; Ittel, S. D. Homogeneous Catalysis. *The Applications and Chemistry of Catalysis by Soluble Transition Metal Complexes*, 2nd ed.; Wiley-Interscience: New York, 1992.
(7) Chirik, P. J.; Wieghardt, K. *Science* **2010**, *327*, 794–795.
(8) Hartwig, J. F. *Organotransition Metal Chemistry—From Bonding to Catalysis*; University Science Books: Sausalito, CA, 2010.
(9) Negishi, E.-I. In *Handbook of Organopalladium Chemistry for Organic Synthesis*; Negishi, E.-I., de Meijere, A., Eds.; Wiley-Interscience: New York, 2002; pp 17−35.
(10) *Metal-Catalyzed Cross-Coupling Reactions*; Diederich, F., Stang, P. J., Eds.; Wiley-VCH: Weinheim, Germany, 1998.
(11) Stahl, S. S. *Science* **2005**, *309*, 1824–1826.
(12) Partenheimer, W. *Catal. Today* **1995**, *23*, 69–158.
(13) Lowry, T. H.; Richardson, K. S. *Mechanism and Theory in Organic Chemistry*; Harper & Row: New York, 1976.
(14) *Biomimetic Oxidations Catalyzed by Transition Metal Complexes*; Meunier, B., Ed.; Imperial College: London, 2000.
(15) Himo, F.; Siegbahn, P. E. M. *Chem. Rev.* **2003**, *103*, 2421–2456.
(16) Whittaker, J. W. *Chem. Rev.* **2003**, *103*, 2347–2363.
(17) Meunier, B.; de Visser, S. P.; Shaik, S. *Chem. Rev.* **2004**, *104*, 3947–3980.
(18) Ortiz de Montellano, P. R. *Cytochrome P450: Structure, Mechanism, and Biochemistry*, 2nd ed.; Plenum Press: New York, 1996.
(19) Pierre, J.-L. *Chem. Soc. Rev.* **2000**, *29*, 251–257.

(20) McGuire, J. R.; Dogutan, D. K.; Teets, T. S.; Suntivich, J.; Shao-Horn, Y.; Nocera, D. G. *Chem. Sci.* **2010**, *1*, 411–414.
(21) Soper, J. D.; Kryatov, S. V.; Rybak-Akimova, E. V.; Nocera, D. G. *J. Am. Chem. Soc.* **2007**, *129*, 5069–5075.
(22) Chng, L. L.; Chang, C. J.; Nocera, D. G. *Org. Lett.* **2003**, *5*, 2421–2424.
(23) Dogutan, D. K.; Stoian, S. A.; McGuire, R.; Schwalbe, M.; Teets, T. S.; Nocera, D. G. *J. Am. Chem. Soc.* **2011**, *133*, 131–140.
(24) Yang, J. Y.; Liu, S.-Y.; Korendovych, I. V.; Rybak-Akimova, E. V.; Nocera, D. G. *ChemSusChem* **2008**, *1*, 941–949.
(25) Crabtree, R. H. *New J. Chem.* **2011**, *35*, 18–23.
(26) Das, S.; Incarvito, C. D.; Crabtree, R. H.; Brudvig, G. W. *Science* **2006**, *312*, 1941–1943.
(27) Borovik, A. S.; Zinn, P. J.; Zart, M. K. In *Activation of Small Molecules: Organometallic and Bioinorganic Perspectives*; Tolman, W. B., Ed.; Wiley-VCH: Weinheim, Germany, 2006; pp 187−234.
(28) Pierpont, C. G. *Coord. Chem. Rev.* **2001**, *216*−*217*, 99–125.
(29) Pierpont, C. G.; Lange, C. W. *Prog. Inorg. Chem.* **1994**, *41*, 331–442.
(30) Blackmore, K. J.; Ziller, J. W.; Heyduk, A. F. *Inorg. Chem.* **2005**, *44*, 5559–5561.
(31) Heyduk, A. F.; Blackmore, K. J.; Ketterer, N. A.; Ziller, J. W. *Inorg. Chem.* **2005**, *44*, 468–470.
(32) Haneline, M. R.; Heyduk, A. F. *J. Am. Chem. Soc.* **2006**, *128*, 8410–8411.
(33) Blackmore, K. J.; Sly, M. B.; Haneline, M. R.; Ziller, J. W.; Heyduk, A. F. *Inorg. Chem.* **2008**, *47*, 10522–10532.
(34) Ketterer, N. A.; Fan, H.; Blackmore, K. J.; Yang, X.; Ziller, J. W.; Baik, M. H.; Heyduk, A. F. *J. Am. Chem. Soc.* **2008**, *130*, 4364–4374.
(35) Zarkesh, R. A.; Ziller, J. W.; Heyduk, A. F. *Angew. Chem., Int. Ed.* **2008**, *47*, 4715–4718.
(36) Nguyen, A. I.; Blackmore, K. J.; Carter, S. M.; Zarkesh, R. A.; Heyduk, A. F. *J. Am. Chem. Soc.* **2009**, *131*, 3307–3316.
(37) Nguyen, A. I.; Zarkesh, R. A.; Lacy, D. C.; Thorson, M. K.; Heyduk, A. F. *Chem. Sci.* **2011**, *2*, 166–169.
(38) Bart, S. C.; Lobkovsky, E.; Bill, E.; Chirik, P. J. *J. Am. Chem. Soc.* **2006**, *128*, 5302–5303.
(39) Bouwkamp, M. W.; Bowman, A. C.; Lobkovsky, E.; Chirik, P. J. *J. Am. Chem. Soc.* **2006**, *128*, 13340–13341.
(40) Bart, S. C.; Bowman, A. C.; Lobkovsky, E.; Chirik, P. J. *J. Am. Chem. Soc.* **2007**, *129*, 7212–7213.
(41) Trovitch, R. J.; Lobkovsky, E.; Chirik, P. J. *J. Am. Chem. Soc.* **2008**, *130*, 11631–11640.
(42) Sylvester, K. T.; Chirik, P. J. *J. Am. Chem. Soc.* **2009**, *131*, 8772–8774.
(43) Russell, S. K.; Milsmann, C.; Lobkovsky, E.; Weyhermuller, T.; Chirik, P. J. *Inorg. Chem.* **2011**, *50*, 3159–3169.
(44) Stanciu, C.; Jones, M. E.; Fanwick, P. E.; Abu-Omar, M. M. *J. Am. Chem. Soc.* **2007**, *129*, 12400–12401.
(45) Chaudhuri, P.; Hess, M.; Mueller, J.; Hildenbrand, K.; Bill, E.; Weyhermueller, T.; Wieghardt, K. *J. Am. Chem. Soc.* **1999**, *121*, 9599–9610.
(46) Chaudhuri, P.; Hess, M.; Weyhermuller, T.; Wieghardt, K. *Angew. Chem., Int. Ed.* **1999**, *38*, 1095–1098.
(47) Mukherjee, C.; Weyhermueller, T.; Bothe, E.; Chaudhuri, P. *Inorg. Chem.* **2008**, *47*, 2740–2746.
(48) Lu, C. C.; Weyhermuller, T.; Bill, E.; Wieghardt, K. *Inorg. Chem.* **2009**, *48*, 6055–6064.
(49) Rolle, C. J.; Hardcastle, K. I.; Soper, J. D. *Inorg. Chem.* **2008**, *47*, 1892–1894.
(50) Smith, A. L.; Soper, J. D. *Polyhedron* **2010**, *29*, 164–169.
(51) Lippert, C. A.; Arnstein, S. A.; Sherrill, C. D.; Soper, J. D. *J. Am. Chem. Soc.* **2010**, *132*, 3879–3892.
(52) Lippert, C. A.; Soper, J. D. *Inorg. Chem.* **2010**, *49*, 3682–3684.
(53) Smith, A. L.; Hardcastle, K. I.; Soper, J. D. *J. Am. Chem. Soc.* **2010**, *132*, 14358–14360.
(54) Espenson, J. H. *Adv. Inorg. Chem.* **2003**, *54*, 157–202.
(55) Yang, X.; Baik, M.-H. *J. Am. Chem. Soc.* **2004**, *126*, 13222–13223.
(56) Yang, X.; Baik, M.-H. *J. Am. Chem. Soc.* **2006**, *128*, 7476–7485.
(57) Lundberg, M.; Blomberg, M. R. A.; Siegbahn, P. E. M. *Inorg. Chem.* **2004**, *43*, 264–274.
(58) Siegbahn, P. E. M.; Crabtree, R. H. *J. Am. Chem. Soc.* **1999**, *121*, 117–127.
(59) Muckerman, J. T.; Polyansky, D. E.; Wada, T.; Tanaka, K.; Fujita, E. *Inorg. Chem.* **2008**, *47*, 1787–1802.
(60) Betley, T. A.; Wu, Q.; Van Voorhis, T.; Nocera, D. G. *Inorg. Chem.* **2008**, *47*, 1849–1861.
(61) Surendranath, Y.; Kanan, M. W.; Nocera, D. G. *J. Am. Chem. Soc.* **2010**, *132*, 16501–16509.
(62) Sameera, W. M. C.; McGrady, J. E. *Dalton Trans.* **2008**, 6141–6149.
(63) Balcells, D.; Raynaud, C.; Crabtree, R. H.; Eisenstein, O. *Chem. Commun.* **2008**, 6610.
(64) Balcells, D.; Raynaud, C.; Crabtree, R. H.; Eisenstein, O. *Inorg. Chem.* **2008**, *47*, 10090–10099.
(65) Schlangen, M.; Schwarz, H. *Dalton Trans.* **2009**, 10155–10165.
(66) Dietl, N.; Engeser, M.; Schwarz, H. *Angew. Chem., Int. Ed.* **2009**, *48*, 4861–4863.
(67) Feyel, S.; Dobler, J.; Schroeder, D.; Sauer, J.; Schwarz, H. *Angew. Chem., Int. Ed.* **2006**, *45*, 4681–4685.
(68) Mayer, J. M. *Acc. Chem. Res.* **1998**, *31*, 441–450.
(69) Mayer, J. M.; Mader, E. A.; Roth, J. P.; Bryant, J. R.; Matsuo, T.; Dehestani, A.; Bales, B. C.; Watson, E. J.; Osako, T.; Valliant-Saunders, K.; Lam, W. H.; Hrovat, D. A.; Borden, W. T.; Davidson, E. R. *J. Mol. Catal. A: Chem.* **2006**, *251*, 24–33.
(70) Mayer, J. M. *Acc. Chem. Res.* **2011**, *44*, 36–46.
(71) France, S.; Wack, H.; Taggi, A. E.; Hafez, A. M.; Wagerle, T. R.; Shah, M. H.; Dusich, C. L.; Lectka, T. *J. Am. Chem. Soc.* **2004**, *126*, 4245–4255.
(72) Bill, E.; Bothe, E.; Chaudhuri, P.; Chlopek, K.; Herebian, D.; Kokatam, S.; Ray, K.; Weyhermueller, T.; Neese, F.; Wieghardt, K. *Chem.—Eur. J.* **2005**, *11*, 204–224.
(73) Poddel'sky, A. I.; Cherkasov, V. K.; Abakumov, G. A. *Coord. Chem. Rev.* **2009**, *253*, 291–324.
(74) Nugent, W. A.; Mayer, J. M. *Metal*−*Ligand Multiple Bonds*; John Wiley & Sons: New York, 1988.
(75) Evans, D. F. *J. Chem. Soc.* **1959**, 2003–2005.
(76) Piguet, C. *J. Chem. Educ.* **1997**, *74*, 815–816.
(77) Cotton, F. A. *Polyhedron* **1987**, *6*, 667–677.
(78) Boehm, G.; Wieghardt, K.; Nuber, B.; Weiss, J. *Inorg. Chem.* **1991**, *30*, 3464–3476.
(79) Differences in solubility necessitated the use of a different solvent. The $Re^{V}_2(\mu\text{-}O)_2(ap^{Ph})_2(isq^{Ph})_2$ dimer is insoluble in CH_3CN.
(80) Chong, D.; Laws, D. R.; Nafady, A.; Costa, P. J.; Rheingold, A. L.; Calhorda, M. J.; Geiger, W. E. *J. Am. Chem. Soc.* **2008**, *131*, 2692–2703.
(81) Connelly, N. G.; Geiger, W. E. *Chem. Rev.* **1996**, *96*, 877–910.
(82) Forrester, A. R.; Hay, J. M.; Thomson, R. H. *Organic Chemistry of Stable Free Radicals*; Academic Press: New York, 1968.
(83) March, J. *Advanced Organic Chemistry: Reactions, Mechanism and Structure*; Wiley-Interscience: New York, 1992.
(84) McBride, J. M. *Tetrahedron* **1974**, *30*, 209–2022.
(85) Holm, R. H. *Chem. Rev.* **1987**, *87*, 1401–1449.
(86) Holm, R. H.; Donahue, J. P. *Polyhedron* **1993**, *12*, 571–589.
(87) DiLabio, G. A.; Ingold, K. U.; Lin, S.; Litwinienko, G.; Mozenson, O.; Mulder, P.; Tidwell, T. T. *Angew. Chem., Int. Ed.* **2010**, *49*, 5982–5985.
(88) Bryant, J. R.; Matsuo, T.; Mayer, J. M. *Inorg. Chem.* **2004**, *43*, 1587–1592.
(89) Steenken, S.; Neta, P. *J. Am. Chem. Soc.* **1982**, *104*, 1244–1248.
(90) Cook, G. K.; Mayer, J. M. *J. Am. Chem. Soc.* **1994**, *116*, 1855–1868.
(91) Cook, G. K.; Mayer, J. M. *J. Am. Chem. Soc.* **1995**, *117*, 7139–7156.

(92) Vanover, E.; Huang, Y.; Xu, L.; Newcomb, M.; Zhang, R. *Org. Lett.* **2010**, *12*, 2246–2249.
(93) Prokop, K. A.; de Visser, S. P.; Goldberg, D. P. *Angew. Chem., Int. Ed.* **2010**, *49*, 5091–5095.
(94) Paine, T. K.; Costas, M.; Kaizer, J.; Que, L., Jr. *J. Biol. Inorg. Chem.* **2006**, *11*, 272–276.
(95) King, E. R.; Hennessy, E. T.; Betley, T. A. *J. Am. Chem. Soc.* **2011**, *133*, 4917–4923.
(96) Wiese, S.; Badiei, Y. M.; Gephart, R. T.; Mossin, S.; Varonka, M. S.; Melzer, M. M.; Meyer, K.; Cundari, T. R.; Warren, T. H. *Angew. Chem., Int. Ed.* **2010**, *49*, 8850–8855.
(97) Badiei, Y. M.; Dinescu, A.; Dai, X.; Palomino, R. M.; Heinemann, F. W.; Cundari, T. R.; Warren, T. H. *Angew. Chem., Int. Ed.* **2008**, *47*, 9961–9964.
(98) Kogut, E.; Wiencko, H. L.; Zhang, L.; Cordeau, D. E.; Warren, T. H. *J. Am. Chem. Soc.* **2005**, *127*, 11248–11249.
(99) Sharp, D. W. A.; Sheppard, N. *J. Chem. Soc.* **1957**, 674–682.
(100) Gomberg, M. *J. Am. Chem. Soc.* **1900**, *22*, 757–771.
(101) *APEX II*; Bruker AXS, Inc., Analytical X-ray Systems: Madison, WI, 2005.
(102) *SAINT*, version 6.45A; Bruker AXS, Inc., Analytical X-ray Systems: Madison, WI, 2003.
(103) Sheldrick, G. M. *Acta Crystallogr.* **2008**, *A64*, 112–122.
(104) *International Tables for X-ray Crystallography*; Wilson, J. C., Ed.; Academic Publishers: Dordrecht, The Netherlands, 1992; Vol. C.